

UNCLASSIFIED

AD NUMBER
AD004240
NEW LIMITATION CHANGE
TO Approved for public release, distribution unlimited
FROM Distribution authorized to U.S. Gov't. agencies and their contractors; Specific Authority; Sep 1952. Other requests shall be referred to WADC, Wright-Patterson, AFB OH.
AUTHORITY
AFAL 1tr 17 Aug 1979

THIS PAGE IS UNCLASSIFIED

53-11-28330

4111 F-2

WADU TECHNICAL REPORT 52-231

SECURITY INFORMATION

~~RESTRICTED~~

~~RESTRICTED~~

CATALOGUED BY WCOSI-3

TI- 4031

Classification cancelled in accordance with
Executive Order 10450 dated 5 November 1953
Low Finley
Document Service Center
Armed Services Tech. Info. Agency
16 Feb 55

DO NOT DESTROY
RETURN TO
TECHNICAL DOCUMENT
CONTROL SECTION
DDO:10

FILE COPY

**AILERON REVERSAL RESEARCH OF STRAIGHT AND SWEEP WINGS
AT HIGH SUBSONIC SPEEDS**

Wright-Patterson
Technical Library
WPAFB, Ohio 45432

**L. GOLAND
CORNELL AERONAUTICAL LABORATORY, INCORPORATED**

SEPTEMBER 1952

WRIGHT AIR DEVELOPMENT CENTER

20011005203

~~RESTRICTED~~
~~RESTRICTED~~

Request
WPAFB
Lang, Dc
app

D-4240

4240

NOTICES

When Government drawings, specifications, or other data are used for any purpose other than in connection with a definitely related Government procurement operation, the United States Government thereby incurs no responsibility nor any obligation whatsoever; and the fact that the Government may have formulated, furnished, or in any way supplied the said drawings, specifications, or other data, is not to be regarded by implication or otherwise as in any manner licensing the holder or any other person or corporation, or conveying any rights or permission to manufacture, use, or sell any patented invention that may in any way be related thereto.

The information furnished herewith is made available for study upon the understanding that the Government's proprietary interests in and relating thereto shall not be impaired. It is desired that the Judge Advocate (WCJ), Wright Air Development Center, Wright-Patterson Air Force Base, Ohio, be promptly notified of any apparent conflict between the Government's proprietary interests and those of others.



This document contains information affecting the National defense of the United States within the meaning of the Espionage Laws, Title 18, U.S.C., Sections 793 and 794. Its transmission or the revelation of its contents in any manner to an unauthorized person is prohibited by law.

RESTRICTED

WADC TECHNICAL REPORT 52-231

RESTRICTED

SECURITY INFORMATION

**AILERON REVERSAL RESEARCH OF STRAIGHT AND SWEEP WINGS
AT HIGH SUBSONIC SPEEDS**

L. Goland

Cornell Aeronautical Laboratory, Incorporated

September 1952

Aircraft Laboratory

Contract W33-038 ac-21174

RDO No. 459-41

Wright Air Development Center
Air Research and Development Command
United States Air Force
Wright-Patterson Air Force Base, Ohio

McGregor & Werner, Inc., Dayton, Ohio
100 - January, 1953

RESTRICTED

RESTRICTED

RESTRICTED

FOREWORD

The research described in this report was conducted at the Cornell Aeronautical Laboratory, Incorporated, Buffalo, New York, under Air Force Contract Number W33-038 ac-21174, with L. Goland as project engineer and W. P. Targoff as Section Head. The project was administered by the Dynamics Branch, Aircraft Laboratory, WADC, under RDO No. 459-41 "General Aeroelastic Studies", with Messrs. W. J. Mykytow and I. N. Spielberg as project engineers. The experimental work was performed in the 8 x 12 foot high speed wind tunnel at Cornell Aeronautical Laboratory.

WADCTR 52-231

RESTRICTED

RESTRICTED

ABSTRACT

Wing and aileron aerodynamic characteristics are obtained from experimental data of wings undergoing the phenomenon of aileron reversal. Wind tunnel tests were conducted on both a straight wing and a 45 degree sweptback wing at Mach numbers of 0.6, 0.7, 0.8 and 0.85.

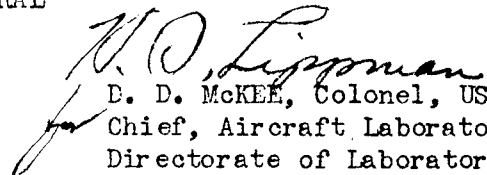
The test results are presented graphically and compared to theoretical and empirical aerodynamic characteristics commonly used in reversal calculations. The characteristics suggested for use by References 1 and 2 are shown to be in reasonably good agreement with the experimental results.

The title of this report is UNCLASSIFIED.

PUBLICATION REVIEW

This report has been reviewed and is approved.

FOR THE COMMANDING GENERAL


D. D. McKee, Colonel, USAF
Chief, Aircraft Laboratory, Acting
Directorate of Laboratories

RESTRICTED

TABLE OF CONTENTS

	Page
I Introduction	1
II Description of Models and Test Equipment	3
III Instrumentation and Calibration	5
IV Description of Test Procedure	7
V Presentation and Reduction of Data	8
VI Discussion of Results	12
VII References	13
Appendix	
A. Sample Calculation - Straight Wing	14
B. Sample Calculation - Swept Wing	15

RESTRICTED

LIST OF ILLUSTRATIONS

Figure		Page
1	Schematic Diagram of Swept Wing Model	17
2	Rolling Moment vs Angle of Attack, Straight Wing	18
3	Pitching Moment vs Angle of Attack, Straight Wing	19
4	(α/δ) Reversal vs Mach No., Straight Wing	20
5	$\partial C_L/\partial \alpha$ vs Mach No., Straight Wing	20
6	Center of Pressure Location vs Mach No., Straight Wing	21
7	Aileron Coefficient, $\partial \alpha/\partial \delta$, vs Mach No., Straight Wing	21
8	Aileron Coefficient, $\partial C_m/\partial \delta$, vs Mach No., Straight Wing	22
9	Distribution of C_l due to Aileron Deflection, Straight Wing	23
10	Rolling Moment vs Angle of Attack, Swept Wing	24
11	Pitching Moment vs Angle of Attack, Swept Wing	25
12	(α/δ) Reversal vs Mach No., Swept Wing	26
13	$\partial C_L/\partial \alpha$ vs Mach No., Swept Wing	26
14	Center of Pressure Location vs Mach No. Swept Wing	27
15	Aileron Coefficient, $\partial \alpha/\partial \delta$, vs Mach No., Swept Wing	27
16	Aileron Coefficient, $\partial C_m/\partial \delta$, vs Mach No., Swept Wing	28
17	Distribution of C_l due to Aileron Deflection, Swept Wing	29
18	Torsional Stiffness vs Roller Position, Straight Wing	30
19	Torsional Stiffness vs Roller Position, Swept Wing	31
20	Straight Wing Model Assembly	32

RESTRICTED

Figure	Page
21 Aileron Control Assembly, Straight Wing	33
22 Variable Torsion Spring Assembly, Aileron Control Motor, Schaevitz Assemblies	34
23 Straight Wing Model Mounted in Wind Tunnel	35
24 Top View of Wind Tunnel Ceiling with Straight Wing Model Installed I	36
25 Top View of Wind Tunnel Ceiling with Straight Wing Model Installed II	37
26 Swept Wing Model Mounted in Wind Tunnel	38
27 Top View of Windtunnel Ceiling with Swept Wing Model Installed I	39
28 Top View of Windtunnel Ceiling with Swept Wing Model Installed II	40
29 Layout of Instrumentation	41

RESTRICTED

SYMBOLS

b	= wing span perpendicular to plane of symmetry of wing (inches).
c	= wing chord measured parallel to plane of symmetry of wing (inches).
\bar{c}	= wing chord measured perpendicular to the leading edge (inches).
S	= model area = $\frac{1}{2}$ wing area (square ft.).
α	= angle of attack measured in plane parallel to plane of symmetry of wing (degrees).
δ	= control surface deflection measured in plane parallel to plane of symmetry of wing (degrees).
$\bar{\delta}$	= control surface deflection measured in plane perpendicular to the leading edge (degrees).
γ	= sweepback angle (degrees).
A	= aspect ratio $(\frac{b^2}{S})$.
M	= Mach number.
q	= free-stream dynamic pressure (lbs. per square foot).
R_e	= Reynold's number based on wing chord parallel to plane of symmetry.
U	= free-stream velocity (feet per second).
M_R	= moment about rolling axis of wing (inch lbs.).
M_p	= moment about pitching axis of wing (inch lbs.).
L	= wing lift (lbs.).
$M_{a.c.}$	= moment about the aerodynamic center due to an aileron deflection (inch lbs.).
$(\frac{\partial C_L}{\partial \alpha})$	= wing lift-curve slope (per radian).
$(\frac{\partial C_L}{\partial \alpha})_\infty$	= two dimensional lift-curve slope of the airfoil section (per radian).
C_L	= section lift coefficient $(\frac{\text{local lift}}{qS})$
$\frac{\partial C_m}{\partial \delta}$	= sectional moment-coefficient slope at zero lift caused by an aileron deflection (per radian).

RESTRICTED

$\left(\frac{\partial C_m}{\partial \delta}\right)_{\delta=0}$ = sectional aileron moment-coefficient slope for straight wing (per radian)

$\left(\frac{\partial \alpha}{\partial \delta}\right)$ = two dimensional aileron effectiveness factor.

η_{cp} = spanwise center of pressure location of one wing panel (fraction of semispan).

\bar{x} = distance from rolling axis to spanwise center of pressure measured perpendicular to plane of symmetry (inches).

\bar{y} = distance from pitching axis to chordwise center of pressure of wing with aileron neutral, measured in plane parallel to plane of symmetry (inches).

a.c. = aerodynamic center location measured in per cent of chord from the leading edge.

e.a. = chordwise position of the elastic axis aft of the leading edge (per cent of chord).

L.E. = refers to leading edge of wing.

RESTRICTED

I INTRODUCTION

The aerodynamic loads imposed upon an aircraft in steady, level flight are of necessity in equilibrium with the internal elastic stresses. The result of raising or lowering an aileron is, effectively, to alter locally the airfoil camber line. The torsional moment produced by this change in camber is resisted by the structural rigidity of the wing. A down aileron produces a moment that decreases the angle of attack of the wing, while an up aileron produces a moment that increases the angle of attack. These induced changes in angle of attack produce airloads which oppose the rolling moment caused by the aileron and thus reduce the effectiveness of the control surface.

As the total aerodynamic torque is approximately proportional to the square of the forward speed of the aircraft, while the resisting elastic torque is independent of this speed, the wing deflections will increase with speed. Therefore, at some speed the change in rolling moment due to the wing twist will be equal in magnitude and opposite in sign to the change in rolling moment due to the aileron deflection. The aileron reversal speed is defined as that speed at which no net change in rolling moment occurs when the ailerons are deflected.

For the straight wing the rolling effectiveness is dependent upon the wing torsional stiffness and independent of the bending stiffness. This results from the fact that bending deformations of a straight wing do not influence the angle of attack distribution. However, in the case of a sweptback wing it is evident that the bending deformation of the wing would influence the angle of attack distribution. This fact increases the complexity of the swept wing problem as compared to the straight wing problem.

Aerodynamically, four wing characteristics, the lift curve slope $\left(\frac{\partial C_L}{\partial \alpha}\right)$, the aileron coefficient $\frac{\partial \alpha}{\partial \delta}$, the moment coefficient at zero lift caused by an aileron deflection $\left(\frac{\partial C_m}{\partial \delta}\right)$, and the aerodynamic center location influence the aileron effectiveness and reversal speed.

The phenomenon of aileron reversal has been treated by numerous investigators and various methods of analysis have been presented. In recent A.M.C. contributions by Groth (References 1 and 2) a number of the methods are listed and analyzed, and methods are proposed for calculating the effectiveness of controls. Also included are empirical values for the aerodynamic coefficients.

Groth concluded that the chief improvement to the simplified calculation would be given by using exact data rather than the empirical values. Consequently, under the cognizance of the Air Materiel Command, wind tunnel tests were conducted to obtain data regarding the behavior of these aerodynamic characteristics within the range of the reversal phenomenon. A straight wing model of aspect ratio 6 (Fig. 23) and a 45 degree sweptback wing model of aspect

RESTRICTED

ratio 3 (Fig. 26) were tested at Mach numbers equal to 0.6, 0.7, 0.8 and 0.85. Both wing models were semi-rigid, having their total flexibility located inboard of the root section. The critical Mach number of the airfoil section (NACA 0008) at zero lift was equal to 0.8.

The first report on these studies (Reference 3) presented the anticipated experimental test conditions, procedures, and models to be utilized. Outside of a few minor changes the tests were conducted as described in Reference (3). The notation of Reference (3), however, has been revised in conformance with that of References (1) and (2).

RESTRICTED

RESTRICTED

II

DESCRIPTION OF MODELS AND TEST EQUIPMENT

A schematic diagram of the model assemblies is shown in Fig. 1, while the actual models and methods of installation are clearly shown in Figs. 20 through 28.

The basic wing models used in these tests were originally used for a high speed flutter investigation (Reference 4). It was necessary to modify these models as the original ones made no provision for ailerons. The models were of semi-rigid cantilever design and had the following properties:

Span: root to tip (parallel to L.E.) = 27" (effective)

Chord (perpendicular to L.E.) = 9"

Thickness = 8%

Aileron Gap = .020"

Airfoil type: modified NACA 0008

Elastic axis aft of L.E. 35% chord

Straight Wing $A = 6$

Swept Wing $A = 3$

The wings were of monocoque construction with 24ST aluminum alloy skin; .064 skin was used on the inboard half of the wing, .032 being used on the outboard end. A solid 24ST aluminum alloy spar of rectangular cross section was provided on the elastic axis and form ribs were fabricated from 24ST bar stock, lightening holes being drilled where practical. The trailing edge was machined from dural stock and the upper and lower skins flush riveted to it. The entire structure was assembled with machine countersunk rivets driven clear through the wing from one surface to the other. A steel end rib and tube were fabricated in one piece, the rib being riveted inside the above described structure near the root. The steel tube protruded beyond the root of the wing and was used for mounting the wing in a universal joint with spring restraint in a "semi-rigid" manner. The aileron was of solid steel construction and was activated by a steel torque rod (Fig. 21). A motor controlled from the instrument panel rotated the torque rod and thereby deflected the aileron (Fig. 22). The aileron was deflected from its neutral position and rigidly held at 3 degrees by providing a stop of proper dimensions against which the torque rod was caused to "wind up". (Fig. 21) This deflection was increased by replacing the 3 degree stop with one of dimensions corresponding to a 6 degree deflection. The wing was so designed that wrinkling of the skin would not occur during the tests and by static tests it was shown that the wing structure and tube could be considered as a rigid body.

The main mounting structure consisted of a "Tee" formed by means of two 6 inch structural steel channels bolted back to back. The foot of this "Tee" was bolted to the wind tunnel ceiling as shown in Figs. 24 and 25 and the two ends of the head were braced by means of steel tube tripods, also shown in the photographs. A universal joint mechanism (Fig. 1) was mounted on the main channel

RESTRICTED

near the wind tunnel ceiling as shown in Fig. 24. The steel tube protruding from the root of the wing was passed through the center of this universal joint and held in place by a pair of lock nuts in such a manner that it was free to rotate about bending and torsional axes passing through the center of the universal joint. The universal joint was so designed, however, that it was capable of taking out any drag loads on the wing.

The two wing types had the same planform area and the same airfoil section normal to the leading edge. The aileron span was 40% of the wing span, while the aileron chord was 20% of the wing chord. Aileron deflections of zero, three and six degrees were obtained while the tunnel was in operation by means of the irreversible control provided by the loaded torque rod.

The semi-rigid wings, as shown in Fig. 1 have their total flexibility located inboard of the root section. Variable torsional stiffness was obtained by means of movable rollers on two cantilever beam springs. Constant bending stiffness was provided by a set of helical springs. Viscous dampers (Figs. 25 and 28) were utilized in order to eliminate any unsteady effects that would tend to be present due to dynamic instability of the models and turbulence in the tunnel. Arrangement of the springs and their controls are shown in the aforementioned photos.

The sweptback configuration was obtained by rotating the entire mounting structure about the root of the wing (Fig. 27). Duplicate channels were provided where attachments were made to the wind tunnel ceiling to allow for the straight and sweptback assembly but all other items of the mounting structure were interchangeable.

With the model mass balanced to zero product of inertia about the bending and torsion axes, analyses of the straight wing revealed that a structural damping coefficient of 0.10 for both the bending and torsion degrees of freedom completely precludes flutter. This damping was provided by the viscous absorbers. However, as a precautionary measure an automatic flutter brake was provided. The flutter brake together with the hydraulic dampers were expected to alleviate any unpredicted vibration phenomenon. However, in agreement with the design flutter analysis, no trouble was experienced due to wing vibrations.

RESTRICTED

III

INSTRUMENTATION AND CALIBRATION

As a result of the tunnel running at approximately $\frac{1}{2}$ atmospheric pressure it was necessary to measure the bending and torsion angular deflections from a point outside of the wind tunnel. These angular deflections, involving maximum rotations of approximately two degrees, were to be determined within $\pm .03$ degrees.

Schaevitz linear differential transformers were selected as the pickup devices. Units with ± 0.190 inch linear travel were used at a six inch arm as shown in Fig. 22. The outputs of the pickoff units were matched against similar units at the operating position (Fig. 29). Indication of correspondence between the pickoff and dummy units was accomplished by means of a null reading meter. As shown in Fig. 29, the dummy unit's core was moved by means of a thumbscrew, and its position was measured by means of an Ames dial indicator, calibrated in ten-thousandths of an inch, having a $\frac{1}{2}$ inch stroke.

The system was first tested by balancing the alternating current outputs of the two Schaevitz units, and indicating null with an A.C. instrument. The required accuracy was not obtained because of the broad null experienced. This was a result of phase shift in the connecting cable, which was approximately 100 ft. in length.

The output of each differential transformer was then rectified and filtered at the unit in such a manner that the polarity was indicative of direction of displacement from the center position. These D.C. voltages were then matched and the difference signal fed through a D.C. amplifier to a zero-center galvanometer. The output was heavily filtered to eliminate any electrical noise due to the vibration of the model which might appear at the output. A lead was brought out to an oscilloscope (Fig. 29) ahead of the filter to show this vibration. A carrier frequency of 100 cps was used to permit observation of oscillations at natural frequencies on the order of 10 cps while minimizing the inductive coupling effects in the measuring circuits.

To eliminate the effect of zero drift of the D.C. amplifier, a motor driven switch alternately short-circuited the input, then reconnected the signal for equal periods, with a frequency of approximately 2 cps. A null was indicated when there was no swing of the galvanometer. The switch used was a telemetering multiplexing switch.

Experience with the system indicated that precision was limited only by repeatability in the mechanical portions of the mechanism. Inasmuch as these parts were themselves quite satisfactory, a high overall accuracy was obtained. (See Page 4).

In order to determine the roller position (on which the torsional stiffness is dependent), the roller carriage drove a potentiometer by means of a steel wire (Fig. 22). This potentiometer, and a dummy located on the control panel (Fig. 29) were connected in a bridge circuit to indicate position in much the same manner as the angular motion pickups.

RESTRICTED

Immediately following the installation of the models in the wind tunnel carts, final calibration checks were made. By use of Ames dials (calibrated in ten-thousandths of an inch), weights, and appropriate lever arm mechanisms the following calibration curves were plotted.

- (1) Dummy Schaevitz deflections versus angular deflections about both the bending and torsion axes. Numerous calibration tests were run and it appeared that the angular deflections could be measured accurately to within $\pm .01$ degrees.
- (2) Dummy potentiometer readings versus torsional spring roller positions.
- (3) Bending moments versus bending deflections.
- (4) Torsional moments versus torsional deflections at various positions of the rollers along the cantilever beams. From these curves the torsional spring constant for each roller position was ascertained. Fig. 18 presents a graph of torsional stiffness versus roller position as used in the straight wing tests. The value of the constant bending stiffness, obtained from curves of (3) above, is also indicated in the aforementioned figure. The results for the swept wing tests are similarly presented in Fig. 19.
- (5) The aileron deflection angles, obtained by inserting the 3 degree and 6 degree stops, were accurately determined. The deflections were found to be 3.07 and 5.92 degrees for the straight wing while the deflections for the swept wing were 3.12 and 6.00 degrees.

In all the above calibration tests only a very small amount of scatter was obtained indicating good mechanical repeatability and high precision.

RESTRICTED

IV

DESCRIPTION OF TEST PROCEDURE

Wind tunnel tests were conducted on a semi-span model of a straight wing of aspect ratio 6 and on a sweptback wing model of aspect ratio 3, at Mach numbers equal to 0.6, 0.7, 0.8 and 0.85. The straight wing tests were conducted during July, 1950 and the swept wing during September, 1950 in the $8\frac{1}{2} \times 12$ ft. Variable Density Tunnel at the Cornell Aeronautical Laboratory.

In order to attain these high subsonic Mach numbers in the C.A.L. wind tunnel, the stagnation pressure was reduced to $\frac{1}{2}$ atmospheric. At each Mach number each wing was tested at a constant Reynolds number, which ranged from $R_e = 1.13 \times 10^6$ to 1.22×10^6 for the straight wing and from $R_e = 1.60 \times 10^6$ to 1.72×10^6 for the swept wing. The average operating dynamic pressures and velocities are listed below for the various Mach numbers.

<u>M</u>	<u>q (lbs. per square foot)</u>	<u>U (feet per second)</u>
0.6	192	675
0.7	228	783
0.8	265	887
0.85	283	950

The greatest deviation of dynamic pressure during a test amounted to 2%.

The straight wing was initially installed in the tunnel at an angle of attack of -0.2 degree while the initial angle of the swept wing was -0.4 degree. The error in flow alignment in the tunnel was negligible. At a given Mach number the angle of attack was controlled simply by varying the torsional stiffness. The torsional and bending deflections were recorded at the various angles of attack until the reversal condition was approached. From the above deflections and the spring calibrations, the rolling and pitching moments were determined at the various angles of attack. The test procedure was as follows.

At zero air speed the torsion spring rollers were set at the maximum stiffness position and the aileron was set in the neutral position. The zero readings were recorded. The tunnel speed was increased to $M = 0.6$. Readings were then recorded as the torsional stiffness was reduced, which increased the magnitude of the angle of attack.

The torsional stiffness was again set at its maximum value and the aileron was deflected to 3 degrees and the above procedure was repeated. Test data were similarly obtained at $M = 0.7, 0.8$ and 0.85 . The tunnel was then shut down and the 6 degree aileron stop was inserted and the procedure repeated. Throughout the tests numerous checks were made on the repeatability of the system which proved to be extremely accurate. The torsional and bending deflection readings were converted to moments during the tests in order to recognize the reversal phenomenon which occurred when $M_D = 0$.

RESTRICTED

V

PRESENTATION AND REDUCTION OF DATA

Data were directly obtained in the form of deflection measurements about the bending and rolling axis, and potentiometer readings indicating the position of the torsional spring roller assembly. From the calibration curves of Schaevitz deflections versus angular deflections, potentiometer readings versus roller position, and the bending and torsion spring calibration curves, the corresponding rolling and pitching moments at various wing angles of attack were determined.

It is recalled that in the swept wing case, the wing angle of attack is a function of both the torsional and bending angular deflections. For the small deflections dealt with herein the relationship is simply $\alpha = \alpha_T \cos \gamma - \alpha_B \sin \gamma$ where α_T and α_B are the torsional and bending deflections respectively. The positive directions of these deflections are indicated in Fig. 1. The moments for the straight wing are presented in Figs. 2 and 3 while those for the swept wing are shown in Figs. 10 and 11. By assuming a spanwise distribution of lift due to wing angle of attack and aileron deflection the above data may be utilized to determine the four aerodynamic coefficients which influence the reversal phenomenon. For the additional (angle of attack) span loading characteristics of both the straight and swept wings the familiar Weissinger method was used. Despite the limitations of a lifting line method such as Weissinger's the good agreement found between experimentally and theoretically determined characteristics warrants confidence in the use of this method to predict the spanwise distribution (Reference 5). To determine the spanwise distribution on the straight wing due to an aileron deflection Reference 6 was used, in which simple computing forms are included for determining this distribution by the Lots method. Use of this method permits the effect of ten semi-span stations to be considered, and the comparisons between a number of theoretical and experimental results have been shown to be extremely good. The resulting distribution for the straight wing at $\alpha = 0$ is shown graphically in Fig. 9. The distribution for the swept wing with an aileron deflected was determined by use of Reference 7 which is based upon the Weissinger method and permits the effect of 4 semi-span stations to be considered. This reference permits the span loading to be rapidly predicted for wings having arbitrary values of sweep and aspect ratio. Considering the compressibility effects (on equivalent aspect ratio and sweep as explained below) at the test Mach numbers, and the accuracy of this method, it appeared to be the most practical for use in the present analysis. It is recalled here that the lift distribution of an airfoil at a given Mach number is obtained by calculating the lift distribution in incompressible flow of an equivalent airfoil the lateral dimensions of which have been reduced in the ratio $\sqrt{1-M^2} : 1$. The aspect ratio is thus reduced in this ratio and the tangent of the sweep angle is increased by $1/\sqrt{1-M^2}$. Thus, the equivalent airfoil aspect ratio and sweep angle varies with Mach number. The resulting distributions for the swept wing at $\alpha = 0$ is shown in Fig. 17.

The above methods have been widely accepted as capable of determining the loading characteristics with accuracy.

With the above conditions, the four aerodynamic characteristics may be determined from the test data by the following equilibrium relationships.

RESTRICTED

Straight Wing

$$\frac{\partial C_L}{\partial \alpha} = \frac{57.3 M_R}{\alpha q S (.148 + \eta_{c.p.})^{b/2}} \quad (1)$$

$$a.c. = (e.a.) - \frac{b/2}{c} \left(\frac{M_P}{M_R} \right) \alpha (.148 + \eta_{c.p.}) \quad (2)$$

where $\eta_{c.p.}$ is the spanwise location of the center of pressure obtained from Reference 5, and the term (.148) accounts for the distance from the wing root to the roll axis (Fig. 1). (M_P/M_R) is the ratio of pitching moment to rolling moment at a given angle of attack given by Figs. 2 and 3.

The aileron coefficients may be determined by use of the spanwise load distribution of Fig. 9 and the relationships:

$$\frac{\partial \alpha}{\partial \delta} = \frac{57.3 M_{R\alpha=0}}{(\partial C_L / \partial \alpha)_{\infty} \delta q S [Area of Fig. 9] (.148 + \eta_{c.p.}^{(a)})^{b/2}} \quad (3)$$

$$\frac{\partial C_m}{\partial \delta} = -2.5 \left\{ (e.a. - a.c.) \left(\frac{\partial C_L}{\partial \alpha} \right)_{\infty} \left(\frac{\partial \alpha}{\partial \delta} \right) [Area of Fig. 9] - \frac{57.3 M_{P\alpha=0}}{q S c \delta} \right\} \quad (4)$$

where $\eta_{c.p.}^{(a)}$ is the spanwise location of the center of pressure for an aileron deflection at $\alpha = 0$, and where $M_{P\alpha=0}$, $M_{R\alpha=0}$ are the corresponding test values of the pitching and rolling moments. In the formulation of Equation

(4) it has been assumed that $\partial C_m / \partial \delta = 0$ outside of the aileron span, since no spanwise distribution of this factor is known and, therefore, the factor 2.5 appears (aileron span 0.4 of wing span).

The determination of the coefficients for $M = 0.6$ is presented in Appendix A as a representative example of the reduction of the test data for the straight wing.

RESTRICTED

Swept Wing

Similar to the treatment of the straight wing, the aerodynamic characteristics of the swept wing may be determined from the following equilibrium relationships:

$$\frac{\partial C_L}{\partial \alpha} = \frac{57.3 (\partial M_R / \partial \alpha)_\delta}{q S (\eta_{c.p.} + .148) b/2} \quad (5)$$

and

$$a.c. = e.a. - (.148 + \eta_{c.p.}) \left[1 + \left(\frac{\partial M_p / \partial \alpha}{\partial M_R / \partial \alpha} \right)_\delta \right] \frac{b}{2c} \quad (6)$$

where $\eta_{c.p.}$ is the spanwise location of the center of pressure obtained from Reference 5.

As difficulty was encountered in controlling the angle of attack of the wing with the aileron in the neutral position no data were recorded for $\delta = 0$.

Nevertheless, the slope of the pitching and rolling moment curves $(\partial M_p / \partial \alpha)_\delta$

and $(\partial M_R / \partial \alpha)_\delta$ with $\delta = 0$ may be assumed the same as those determined at any constant aileron deflection and, therefore, these values may be obtained from the curves of Figs. 10 and 11.

The aileron coefficients may be determined by use of the relationships,

$$M_{p_{\alpha=0}} = M_{a.c.} \cos \gamma - L \bar{y} \quad (7)$$

$$M_{R_{\alpha=0}} = M_{a.c.} \sin \gamma + L \bar{x} \quad (8)$$

$$\text{where } M_{a.c.} = 0.4 \frac{\partial C_m}{\partial \delta} \bar{\delta} q S \bar{c}$$

$$L = \frac{\partial \alpha}{\partial \delta} \bar{\delta} [\text{Area of Fig. 17}] q S \quad (9)$$

$$\bar{x} = (.148 + \eta_{c.p.}^{(a)}) b/2$$

$$\text{and } \bar{y} = \bar{x} - (.35 - a.c.) c$$

RESTRICTED

Swept Wing - contd.

In the aforementioned expressions $\eta_{c.p.}$ is the spanwise location of the center of pressure due to an aileron deflection at $\alpha = 0$. This location is indicated in Fig. 17 which shows the spanwise distribution of the lift at $\alpha = 0$ for the two extreme cases of $M = 0.6$ and 0.85 as determined by use of Reference 7. The factor 0.4 is again introduced as previously explained. With the two simultaneous Equations (7) and (8), the values of $\partial C_m / \partial \delta$ and $\partial \alpha / \partial \delta$ may be ascertained.

The determination of the coefficients for $M = 0.85$ is presented in Appendix B as a representative example of the reduction of the test data for the swept wing.

RESTRICTED

VI

DISCUSSION OF RESULTS

The test results for the straight wing are shown graphically in Figs. 4 through 8, while the swept wing results are shown in Figs. 12 through 16.

In general, it is noticed that below the critical Mach number, the empirical values of the aerodynamic characteristics presented in References (1) and (2) agree favorably with the test results. Above the critical Mach number the experimental results differ from the predicted values. The critical Mach number of the straight wing is approximately 0.8 while that for the swept wing is above 0.85.

The value of (α/δ) at reversal, as shown in Fig. 4 agrees favorably with the value predicted in Reference (3) by use of a highly simplified method. Similarly, for the swept wing, agreement also appears favorable as shown in Fig. 12.

It can be seen from Figs. 5 and 13 that the lift curve slope predicted by use of the Weissinger method (Reference 5) is in good agreement with the test results. However, while predicting the total lift accurately it may be noticed (Figs. 6 and 14) that appreciable discrepancy exists in the chordwise location of the aerodynamic center. The Weissinger method, being a modified lifting line method, assumes the aerodynamic center at 0.25 chord. The test results indicate a slight tendency of the aerodynamic center to move forward with increasing Mach number. This tendency is in agreement with a recent paper (Reference 8) which is more accurate for predicting chordwise pressure distributions of low aspect ratio wings than is the Weissinger method. Fortunately, however, the error in chordwise position of the aerodynamic center seems to have small effect on the determination of the reversal speed and appears not to be a serious argument against use of this method for reversal calculations. In fact, Reference (1) indicates that in the first approximation the distance (e. a. - a. c.) may be assumed to be zero. An illustrative example in the aforementioned reference indicates that the reversal speed as determined with this assumption is conservative by less than $\frac{1}{2}\%$ for every 10% of chord which the elastic axis lies behind the aerodynamic center.

The variations of the aileron coefficients $\partial a/\partial \delta$ and $\partial C_m/\partial \delta$ with Mach number are shown plotted in Figs. 7 and 8 for the straight wing, while Figs. 15 and 16 show the swept wing variations. The effect on the reversal speed of using the empirical rather than the exact aileron coefficients is discussed in Reference (2) and an example therein indicates that large errors may be introduced by use of the empirical values, especially in the transonic region.

RESTRICTED

VII

REFERENCES

1. Groth, E. EVALUATION OF METHODS FOR CALCULATING THE ROLLING EFFECTIVENESS AND AILERON REVERSAL SPEED OF A STRAIGHT WING A.M.C. MCREXA5
4595-8-6 (December 1948)
2. Groth, E. DETERMINATION OF THE ROLLING EFFECTIVENESS AND AILERON REVERSAL SPEED OF AN ELASTIC SWEEP WING A.M.C. MCREXA5 4595-8-10
(October 1949)
3. Goland, L. INTERIM REPORT ON AILERON REVERSAL RESEARCH Cornell
Aeronautical Laboratory Report SB-569-S-1 (August 1949)
4. Curtiss-Wright Corporation Report No. H-47-3 (September 1947)
RESTRICTED
5. DeYoung, John THEORETICAL ADDITIONAL SPAN LOADING CHARACTERISTICS OF WINGS WITH ARBITRARY SWEEP, ASPECT RATIO, AND TAPER RATIO TN 1491
(December 1947)
6. Pearson, H. A. SPAN LOAD DISTRIBUTION FOR TAPERED WINGS WITH PARTIAL SPAN FLAPS N.A.C.A. Report No. 585 (1937)
7. Stevens, Victor I. THEORETICAL BASIC SPAN LOADING CHARACTERISTICS OF WINGS WITH ARBITRARY SWEEP, ASPECT RATIO, AND TAPER RATIO N.A.C.A.
TN 1772 (December 1948)
8. Lawrence, H. R. THE LIFT DISTRIBUTION ON LOW ASPECT RATIO WINGS AT SUBSONIC SPEEDS I.A.S. Preprint No. 313 (1951)
9. Glauert, H. AEROFOIL AND AIRSCREW THEORY Cambridge University Press
(1942)

RESTRICTED

APPENDIX

A. Straight Wing

The aerodynamic characteristics are determined below for $M = 0.6$.

From Fig. 2, the rolling moment is -450 in. lbs. at $\alpha = -1$ and $\delta = 0$. The spanwise location of the center of pressure for this Mach number is given in Reference 5 as $\eta_{c.p.} = 0.454$. Applying Equation (1),

$$\frac{\partial C_L}{\partial \alpha} = \frac{57.3 (450)}{(192) 1.69 (.148 + .454) 27} = 4.90 \text{ per radian.}$$

The corresponding pitching moment at $\alpha = -1$ and $\delta = 0$ is given in Figs. 3 as 35 in. lbs. Thus from Equation (2)

$$a.c. = 0.35 - \frac{27}{9} \left(\frac{35}{450} \right) (.148 + .454) = 0.21$$

The rolling moment due to aileron alone ($\alpha = 0$, $\delta = 3.07$) is 350 in. lbs. as shown in Fig. 2. The area of Fig. 9 is 0.336 and $\eta_{c.p.}^{(a)} = 0.596$. The two

dimensional section lift coefficient $(\partial C_L / \partial \alpha)_{\infty}$ can be accurately determined from the wing lift coefficient by the expression,

$$\frac{\partial C_L}{\partial \alpha} = \frac{\left(\frac{\partial C_L}{\partial \alpha} \right)_{\infty}}{1 + \left(\frac{\partial C_L}{\partial \alpha} \right)_{\infty} \frac{25}{\pi b^2} (1 + \tau)}$$

where the parameter τ (which accounts for taper ratio) is given in Fig. 88 of Ref. 10 as equal to 0.17 for the subject wing. Applying the above expression there results

$$\left(\frac{\partial C_L}{\partial \alpha} \right)_{\infty} = 7.05$$

and finally Equation (3) yields;

$$\frac{\partial \alpha}{\partial \delta} = \frac{57.3 (350)}{7.05 (3.07) 192 (1.69) 0.336 (0.744) 27} = 0.424$$

RESTRICTED

The corresponding pitching moment due to an aileron deflection alone ($\alpha = 0$, $\delta = 3.07$) is -23 in lbs. (Fig. 3). Accordingly Equation (4) gives

$$\frac{\partial C_m}{\partial \delta} = -2.5 \left\{ (.35 - .21) 7.05 (4.24) 0.336 + \frac{57.3 (23)}{192 (1.69) 9 (3.07)} \right\}$$

$$= -0.72 \text{ per radian}$$

B. Swept Wing

The aerodynamic characteristics are determined below for $M = 0.85$.

From Fig. 10 at $M = 0.85$, the average slope of the rolling moment curves is $(\partial M_R / \partial \alpha)_\delta = 290$ in. lbs. per degree. The spanwise location of the center of pressure is $\eta_{c.p.} = 0.458$ (Reference 5). Consequently, Equation (5) yields,

$$\frac{\partial C_k}{\partial \alpha} = \frac{57.3 (290)}{283 (1.69) (.458 + .148) 19.1} = 3.00 \text{ per radian}$$

$(\partial M_P / \partial \alpha)_\delta$ and $(\partial M_R / \partial \alpha)_\delta$ are equal to 238 in. lbs. per degree and 290 in. lbs.

per degree respectively (Figs. 10 and 11). Reference 5 shows that $\eta_{c.p.} = 0.458$. Thus, according to Equation (6),

$$a.c. = 0.35 - (0.148 + 0.458) \left[1 - \frac{238}{290} \right] \frac{19.1}{12.7} = 0.185$$

RESTRICTED

By use of Equations (9) and Fig. 17 there is obtained,

$$M_{a.c.} = 0.4 \frac{\partial C_m}{\partial \delta} \frac{6}{57.3} (283) 1.69 (9)$$

$$= 180 \frac{\partial C_m}{\partial \delta} \text{ in. lbs.}$$

$$L = \frac{\partial \alpha}{\partial \delta} \frac{6(707)}{57.3} [0.82] 283 (1.69)$$

$$= 34.8 \frac{\partial \alpha}{\partial \delta} \text{ lbs.}$$

$$\bar{x} = (0.140 + 0.612) 19.1 = 14.5 \text{ inches}$$

$$\bar{y} = 14.5 - (.35 - .185) 12.7 = 12.4 \text{ inches}$$

By use of Equations (7) and (8) and Figs. 10 and 11 ($\alpha = 0$, $\delta = 6^\circ$),

$$-228 = 127 \frac{\partial C_m}{\partial \delta} - 431 \frac{\partial \alpha}{\partial \delta}$$

$$194 = 127 \frac{\partial C_m}{\partial \delta} + 305 \frac{\partial \alpha}{\partial \delta}$$

and these simultaneous equations finally yield

$$\frac{\partial \alpha}{\partial \delta} = 0.450$$

$$\frac{\partial C_m}{\partial \delta} = -0.268$$

RESTRICTED

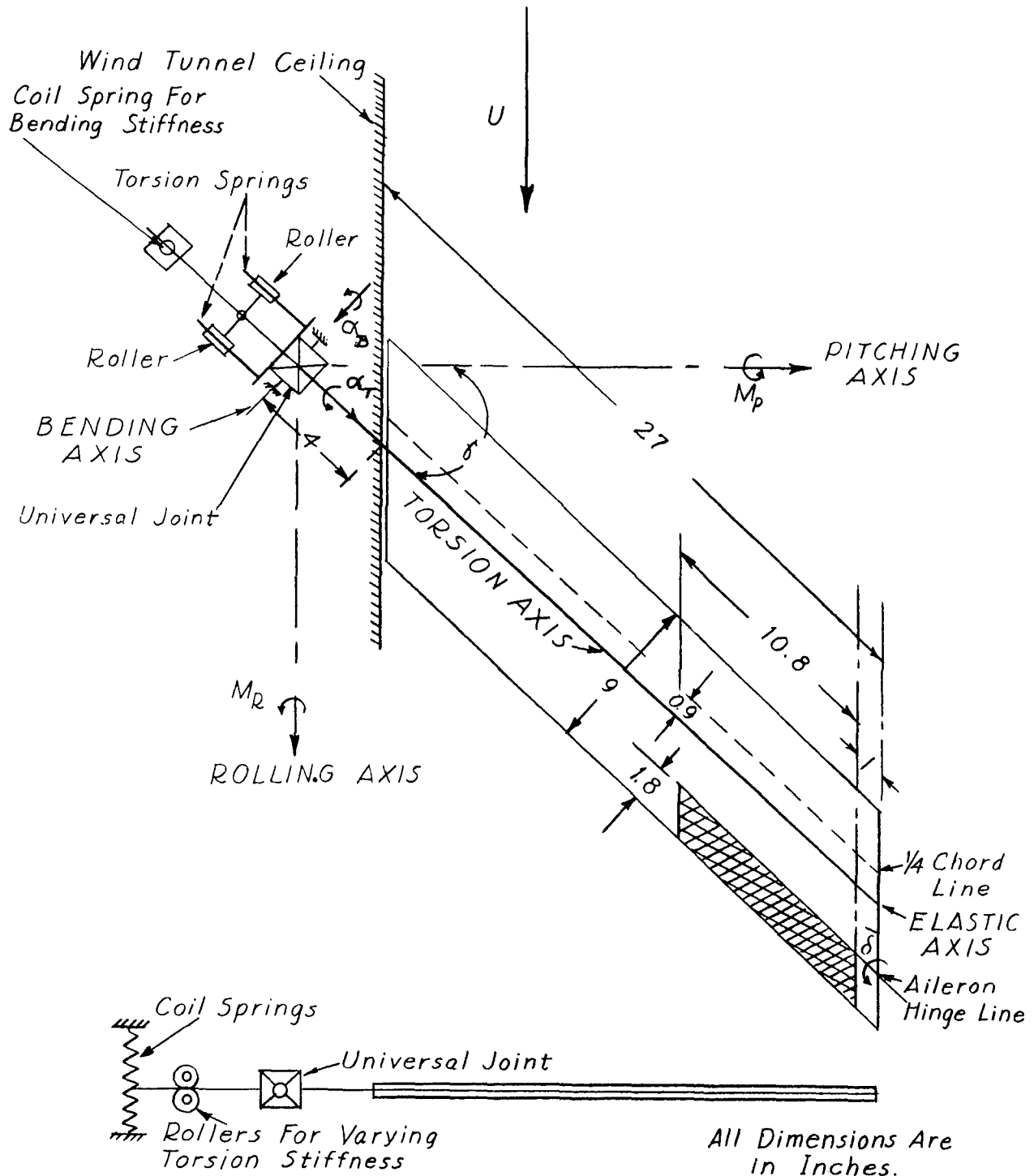


Fig. 1 - SCHEMATIC DIAGRAM OF
SWEEP WING MODEL

RESTRICTED

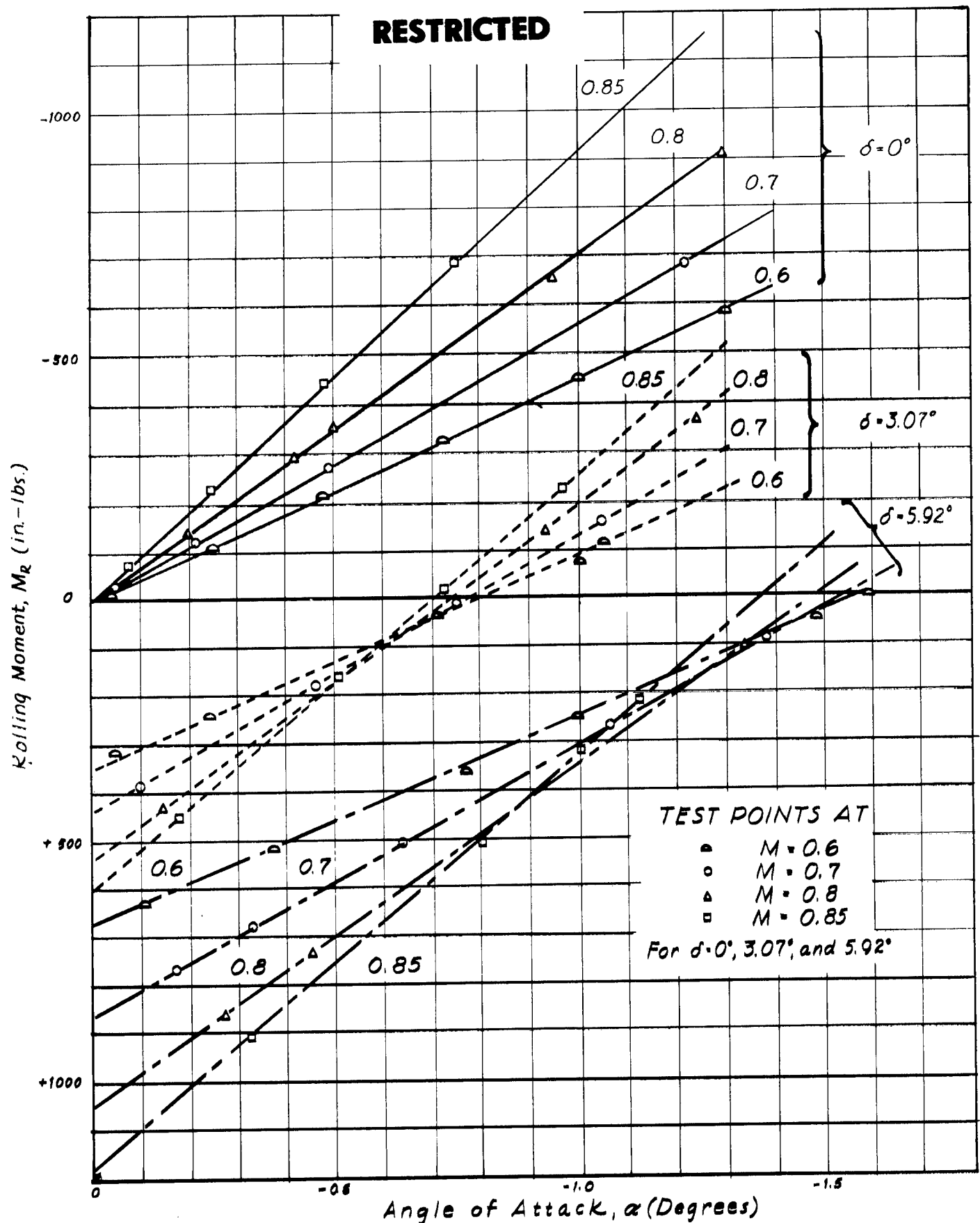


Fig. 2- ROLLING MOMENT vs. ANGLE OF ATTACK
STRAIGHT WING
RESTRICTED

RESTRICTED

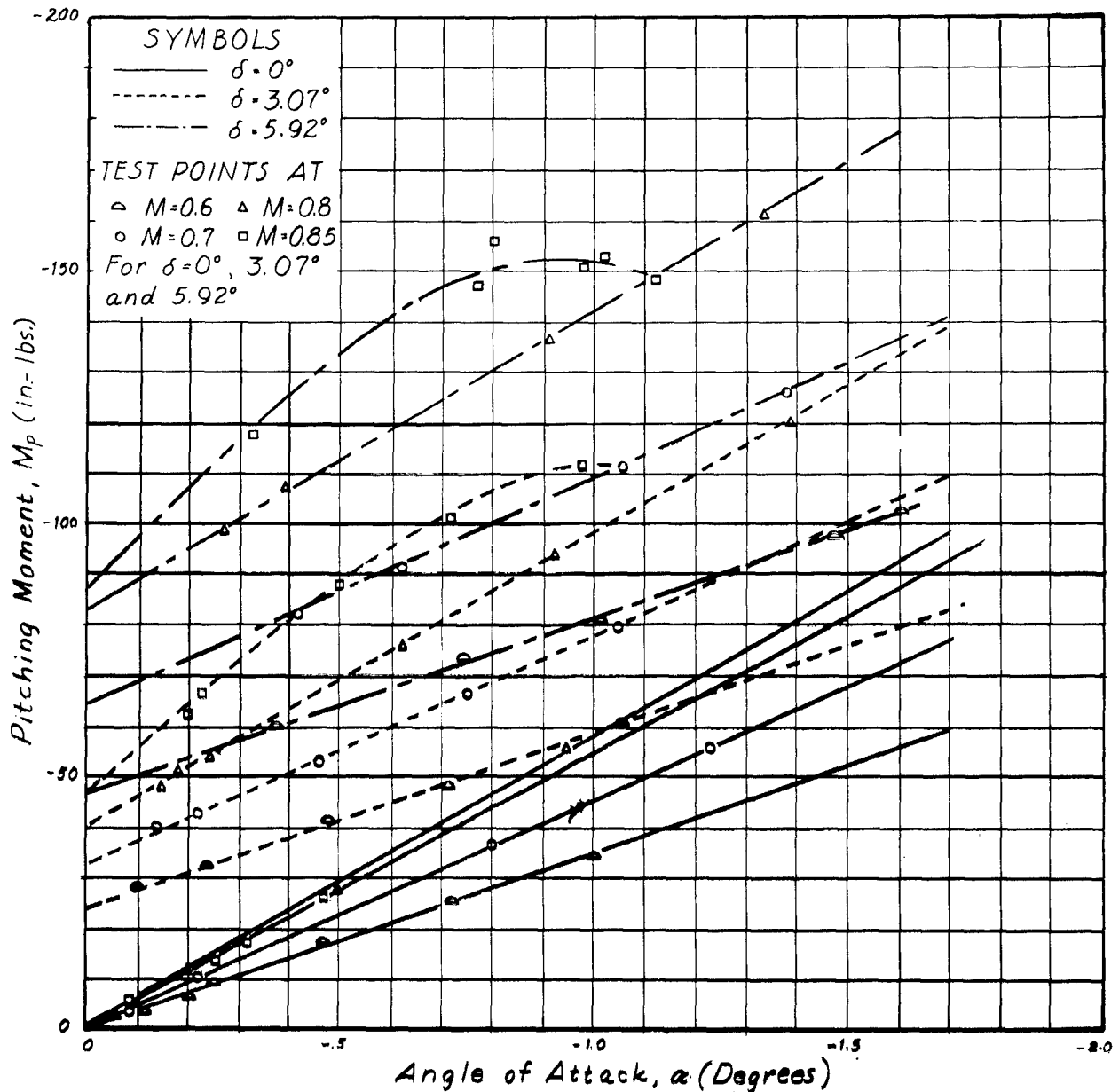


Fig. 3 - PITCHING MOMENT vs. ANGLE OF ATTACK
STRAIGHT WING

RESTRICTED

RESTRICTED

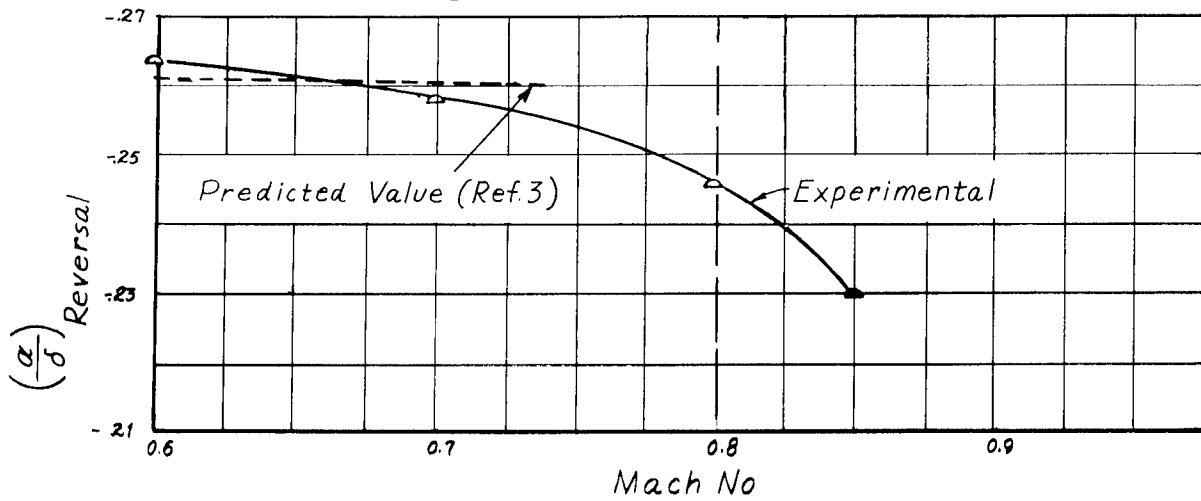


Fig. 4 - $(\frac{\alpha}{\delta})_{\text{Reversal}}$ vs MACH NO.
STRAIGHT WING

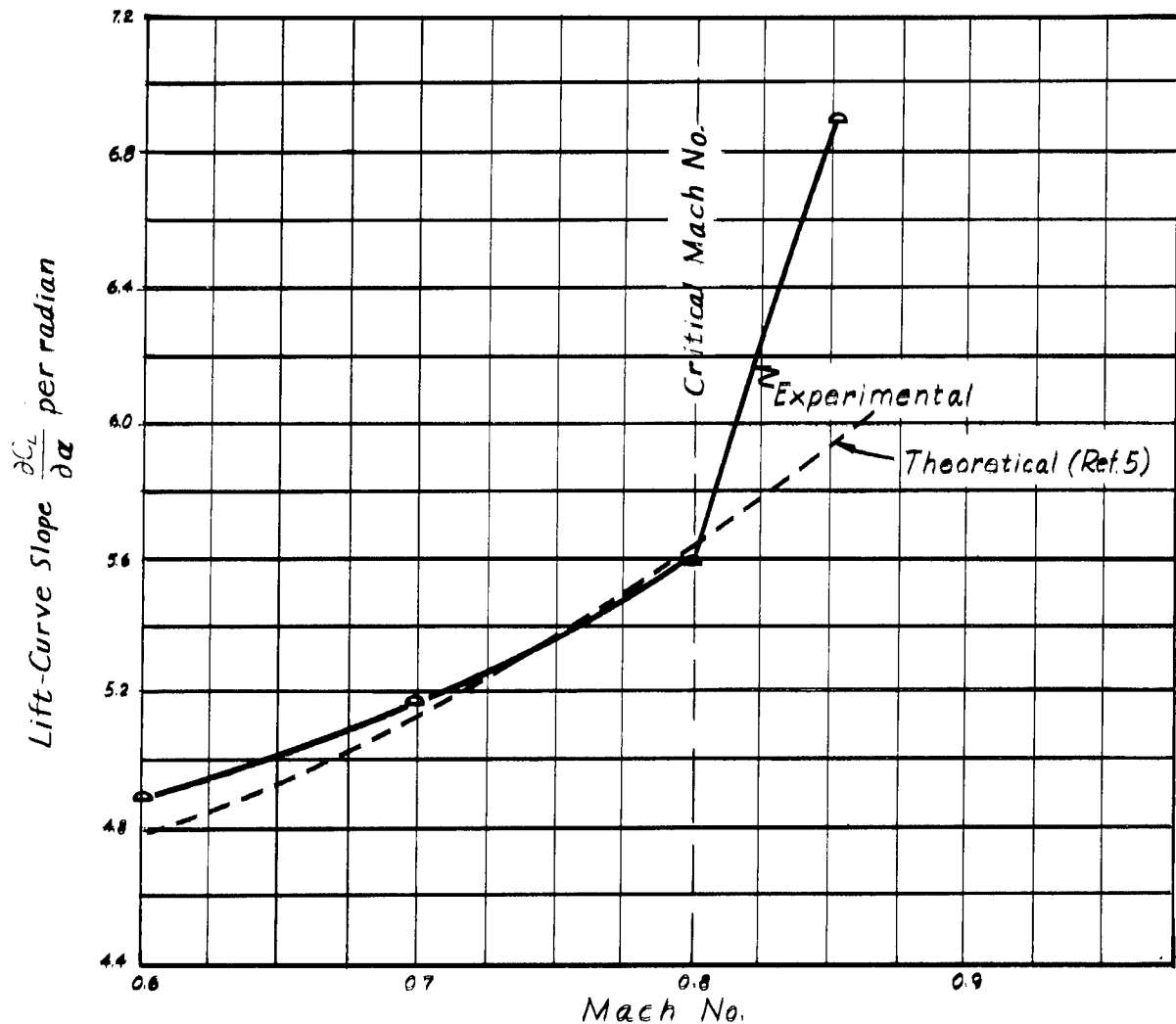


Fig. 5 - $\frac{\partial C_L}{\partial \alpha}$ vs MACH NO.
STRAIGHT WING

RESTRICTED

RESTRICTED

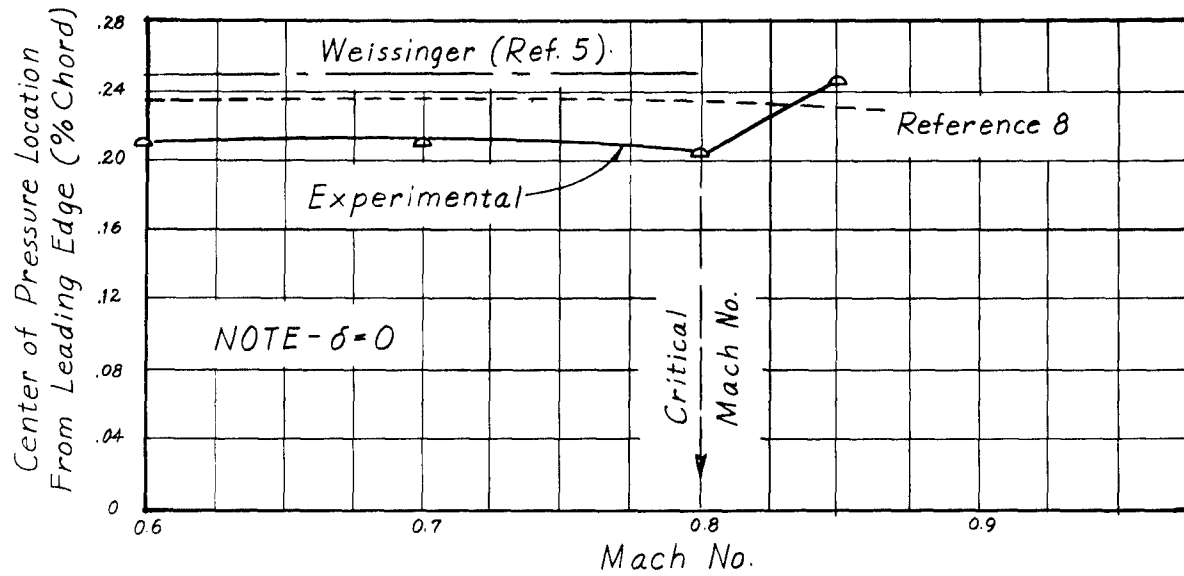


Fig. 6 - CENTER OF PRESSURE LOCATION vs. MACH NO.
STRAIGHT WING

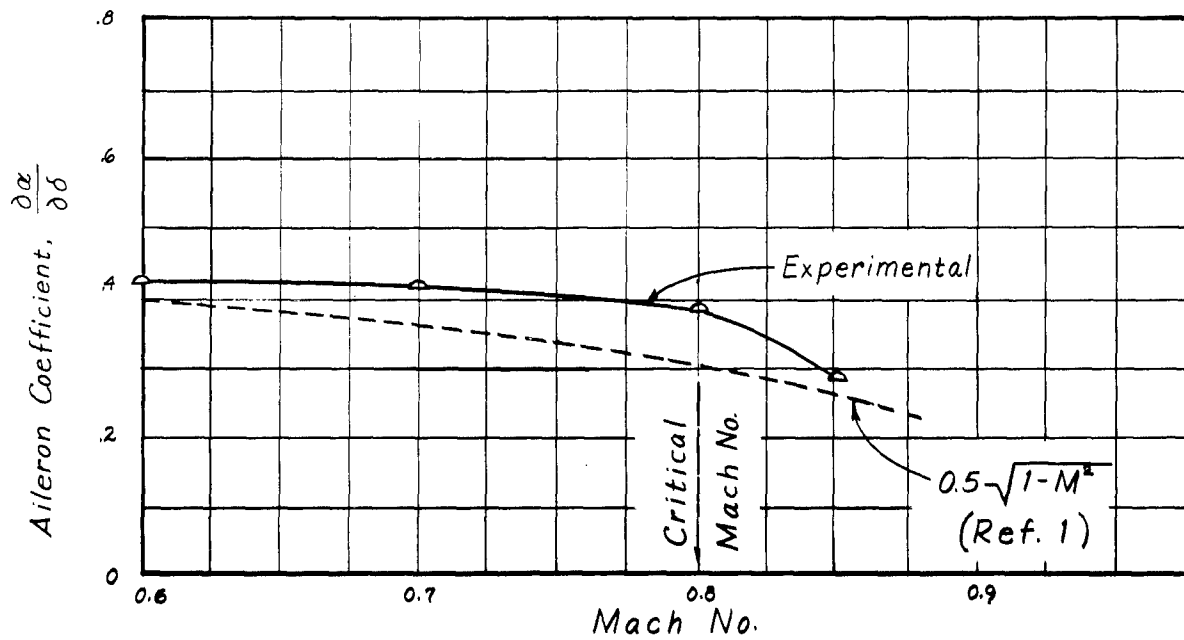


Fig. 7 - AILERON COEFFICIENT, $\frac{\partial \alpha}{\partial \delta}$, vs. MACH NO.
STRAIGHT WING

RESTRICTED

RESTRICTED

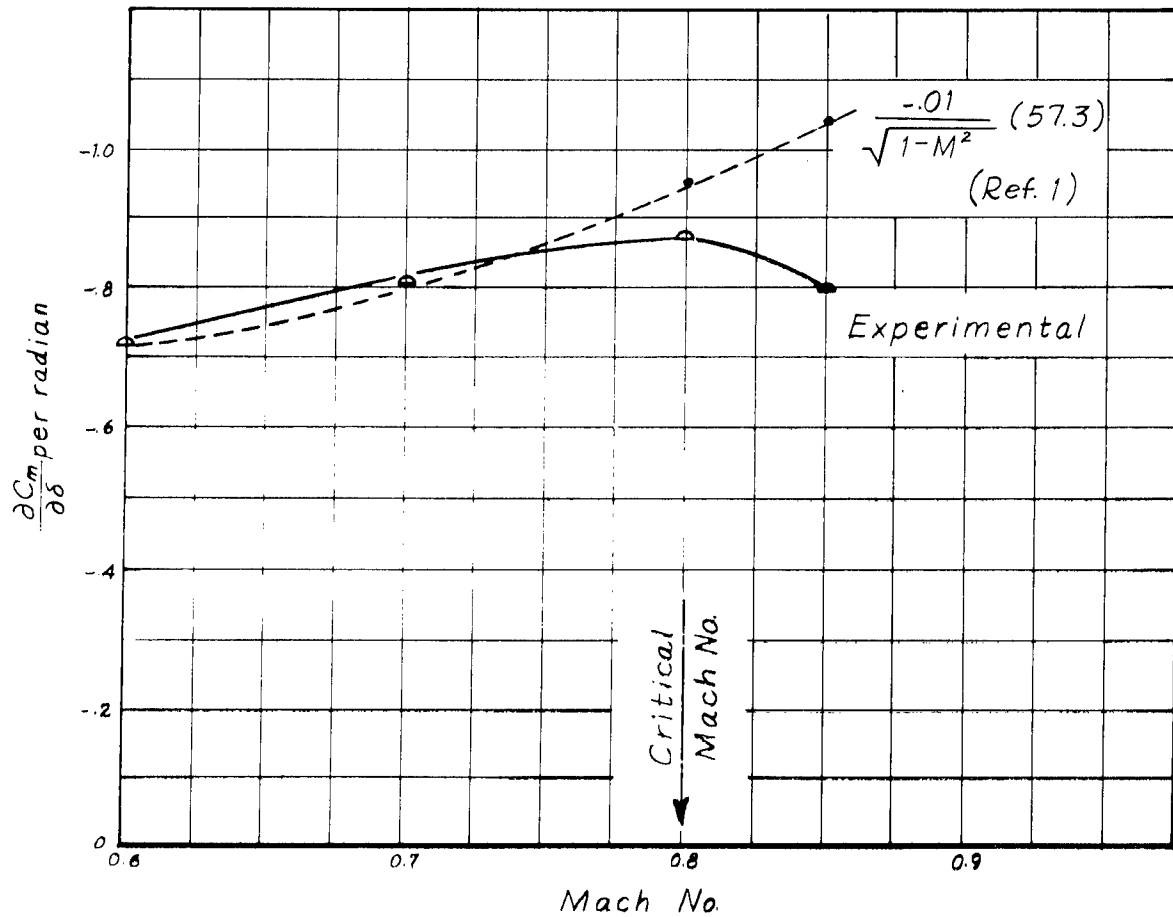


Fig. 8-AILERON COEFFICIENT, $\frac{\partial C_m}{\partial \delta}$, vs. MACH NO.
STRAIGHT WING

RESTRICTED

RESTRICTED

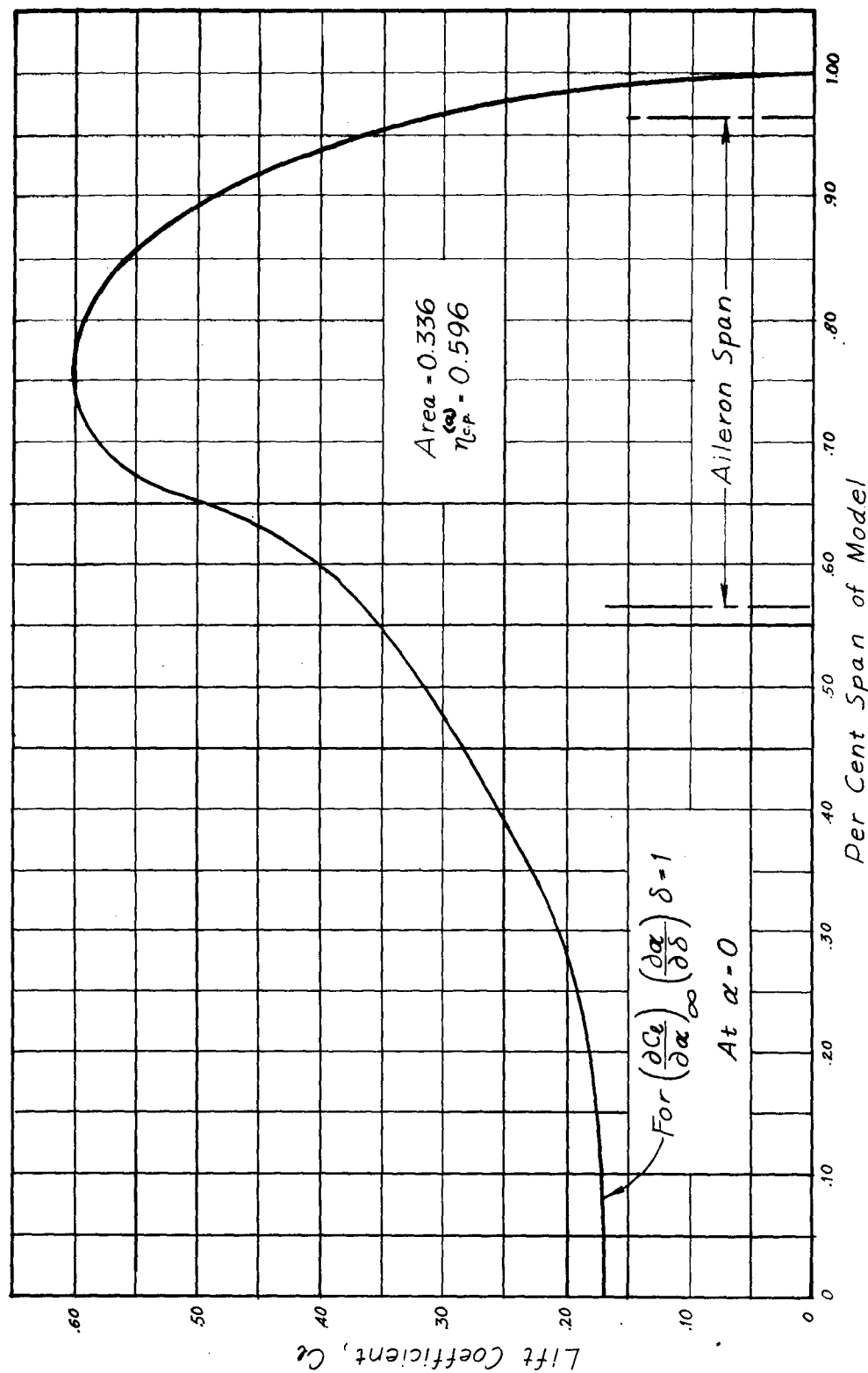


Fig. 9 - DISTRIBUTION OF C_L DUE TO AILERON DEFLECTION STRAIGHT WING

RESTRICTED

RESTRICTED

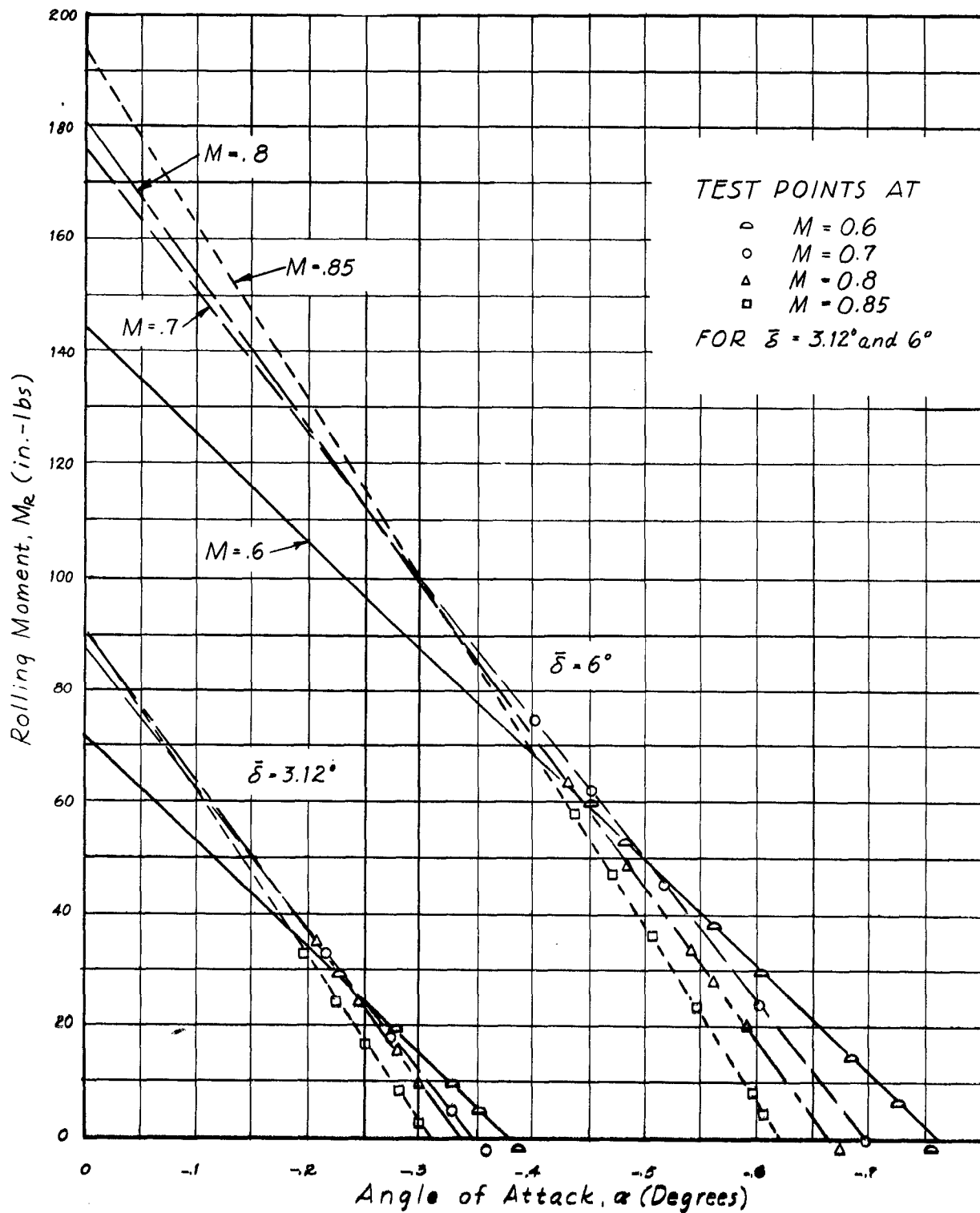


Fig. 10- ROLLING MOMENT vs ANGLE OF ATTACK
SWEEP WING

RESTRICTED

RESTRICTED

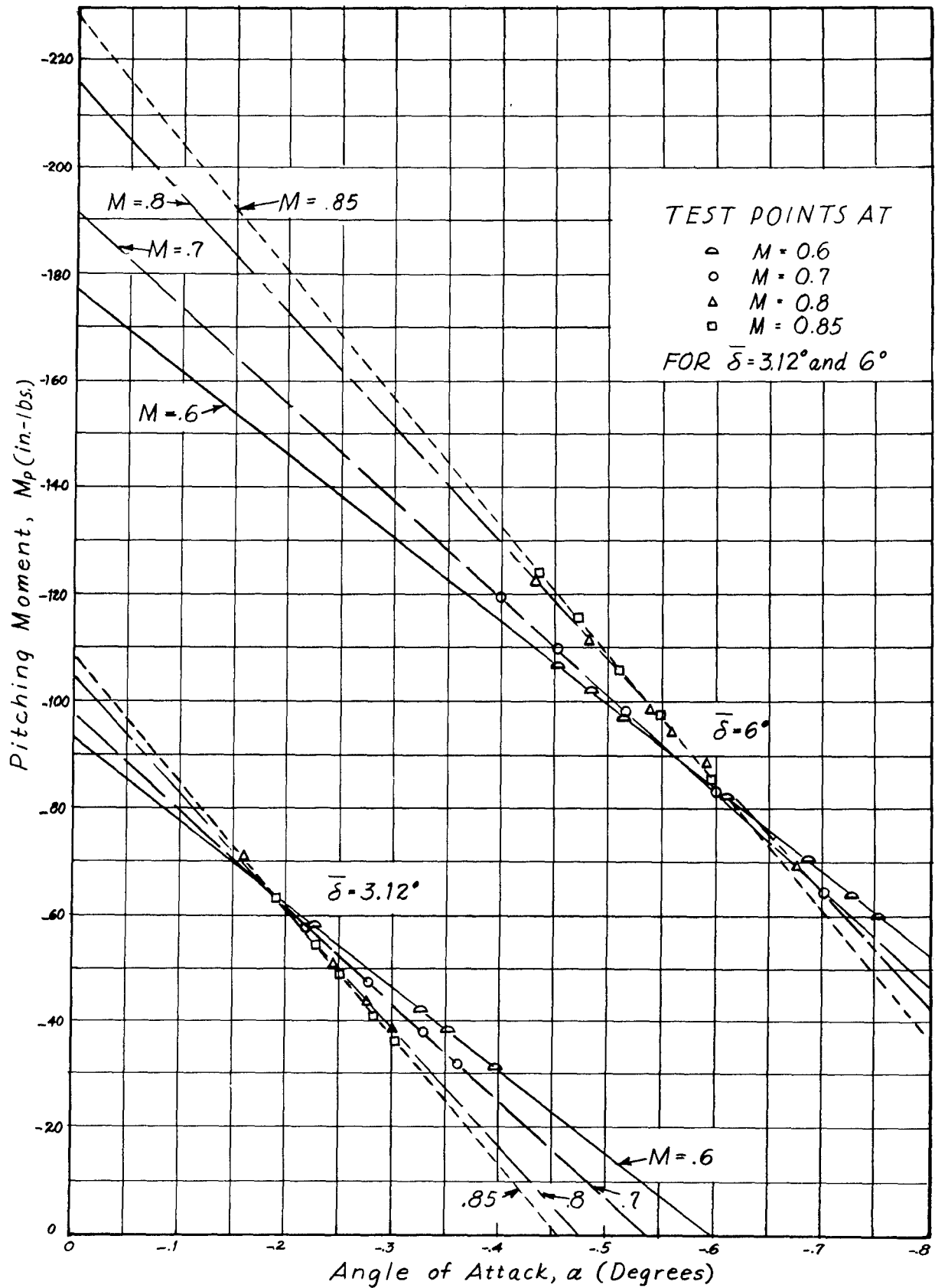


Fig. 11- PITCHING MOMENT vs. ANGLE OF ATTACK
SWEEP WING

RESTRICTED

RESTRICTED

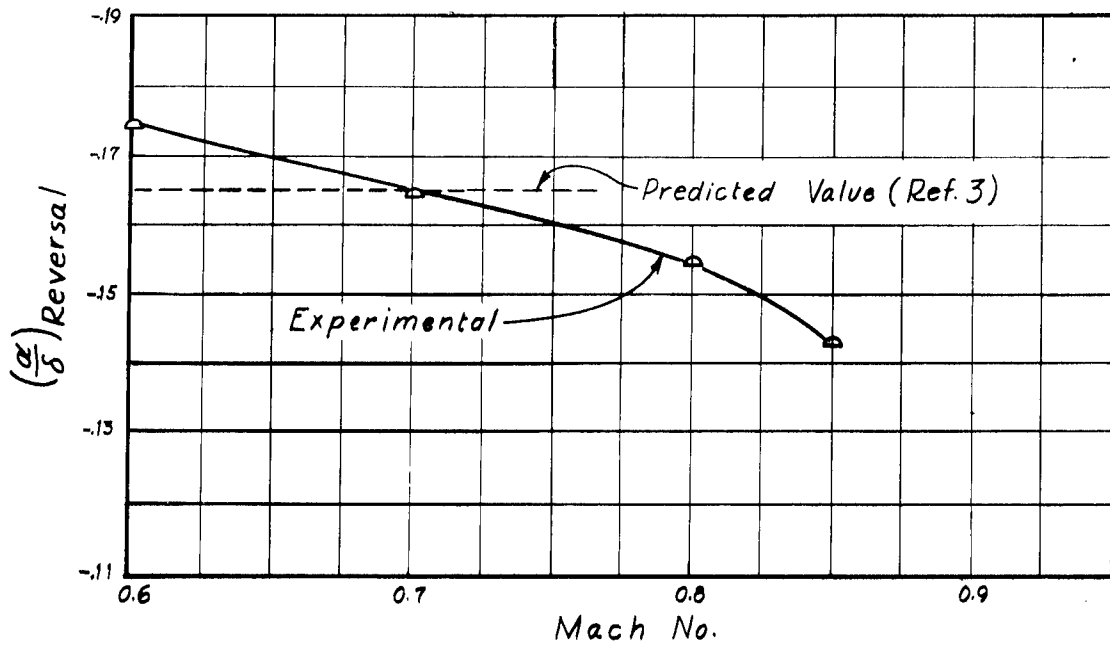


Fig. 12- $(\frac{\alpha}{\delta})_{\text{Reversal}}$ vs MACH NO.
SWEPT WING

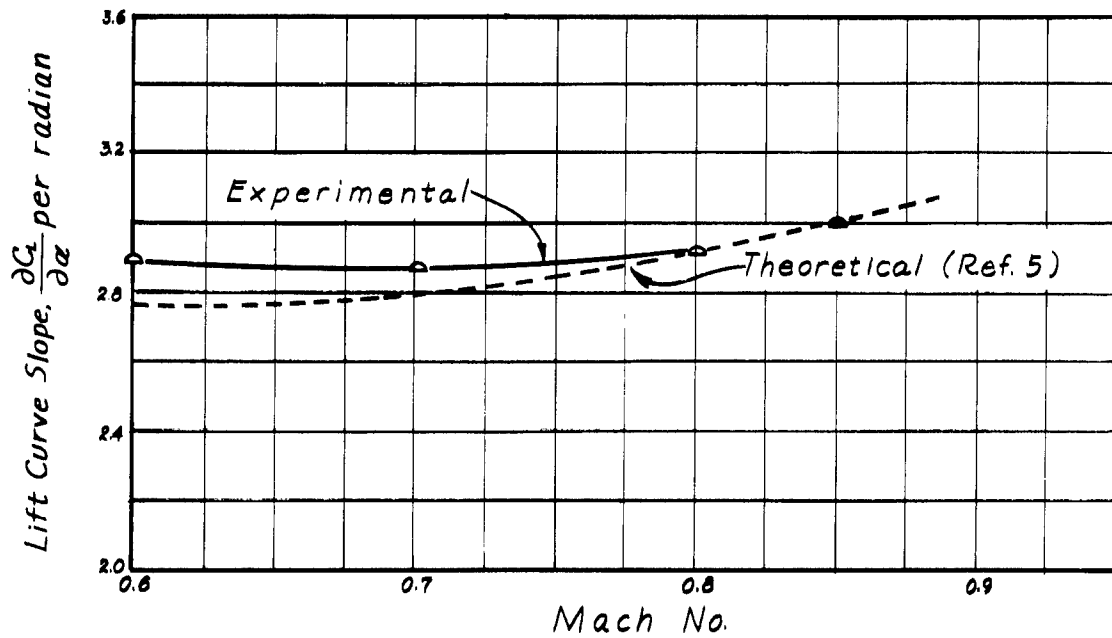


Fig. 13- $\frac{\partial C_L}{\partial \alpha}$ vs MACH NO.
SWEPT WING

RESTRICTED

RESTRICTED

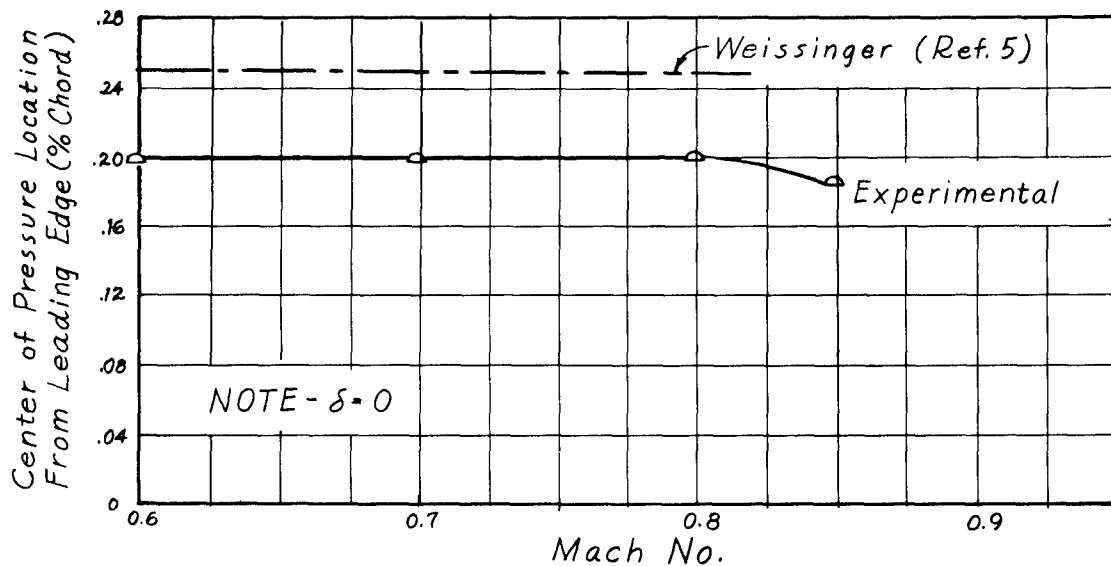


Fig. 14- CENTER OF PRESSURE LOCATION vs MACH NO.
SWEPT WING

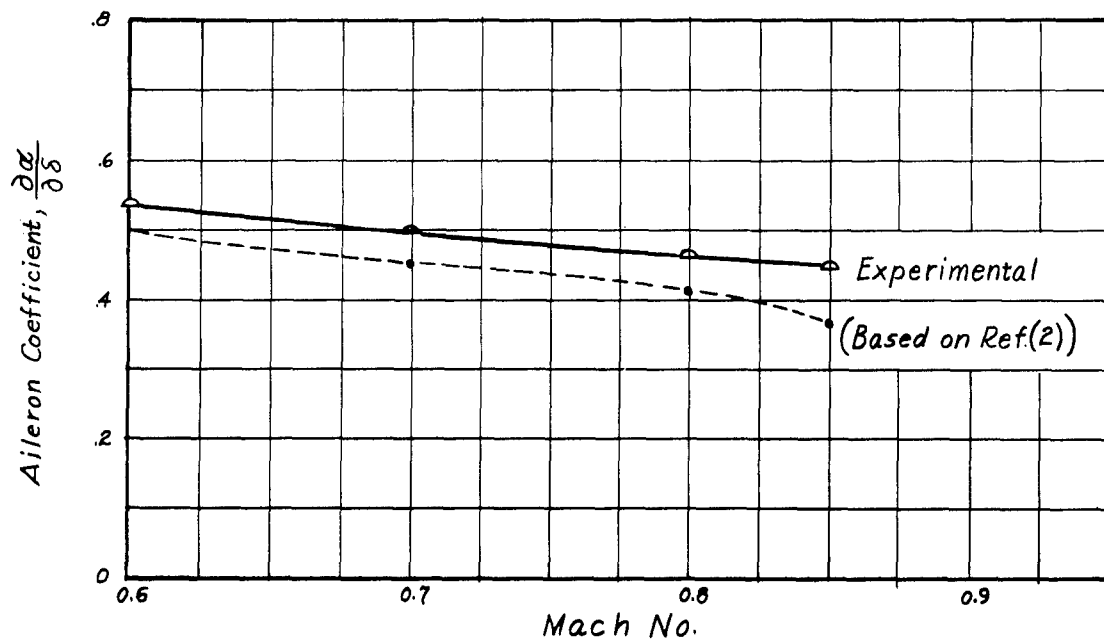


Fig. 15- AILERON COEFFICIENT, $\frac{\partial a}{\partial \delta}$, vs. MACH NO.
SWEPT WING

RESTRICTED

RESTRICTED

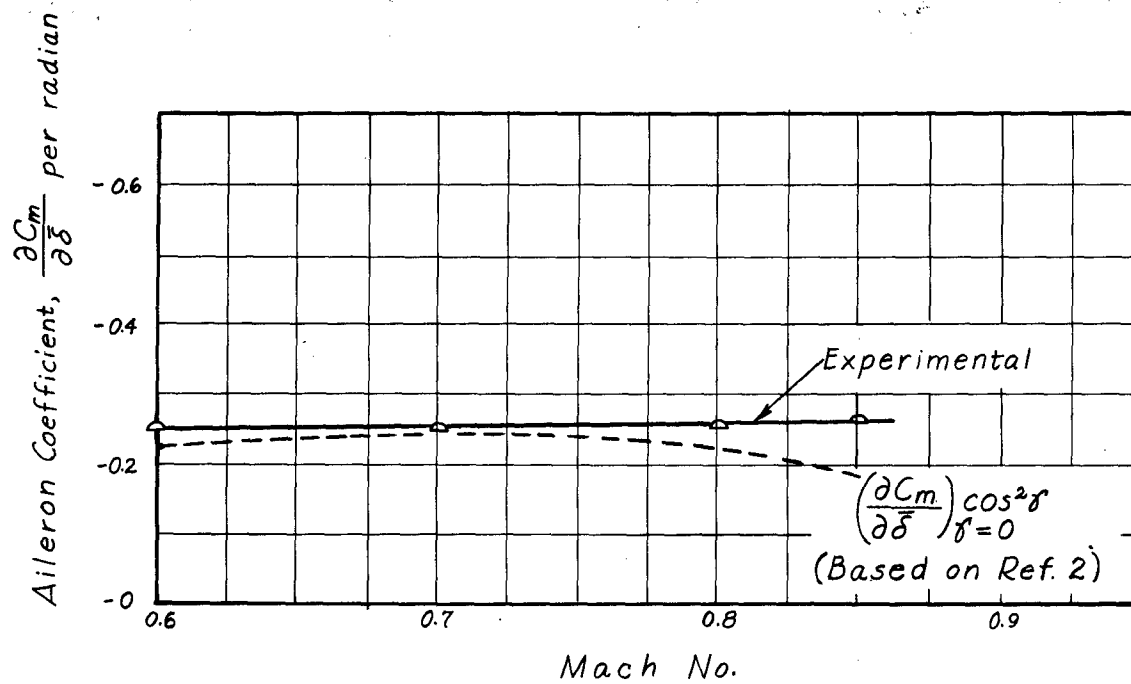


Fig. 16-AILERON COEFFICIENT,
 $\frac{\partial C_m}{\partial \delta}$, vs. MACH NO.
SWEPT WING

RESTRICTED

RESTRICTED

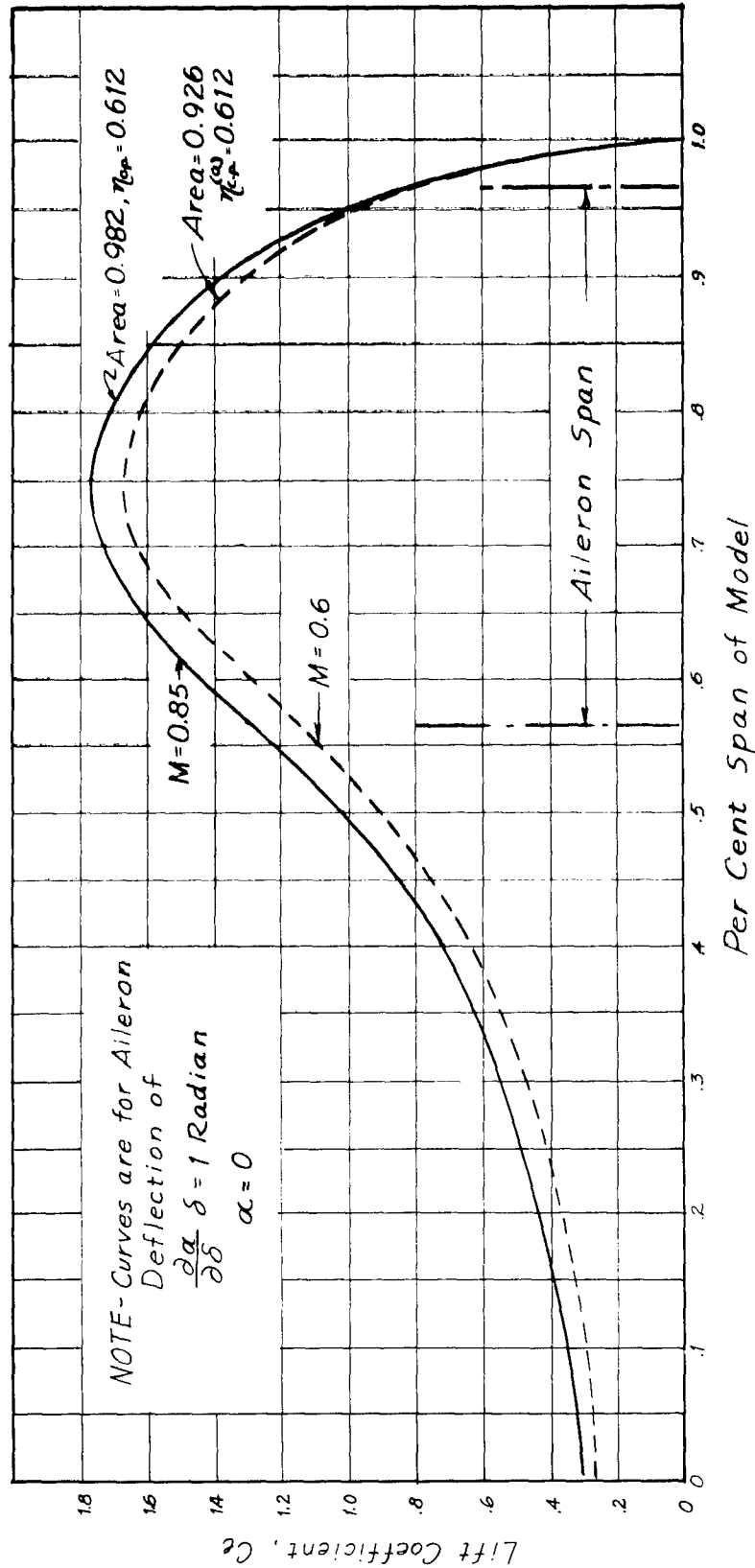
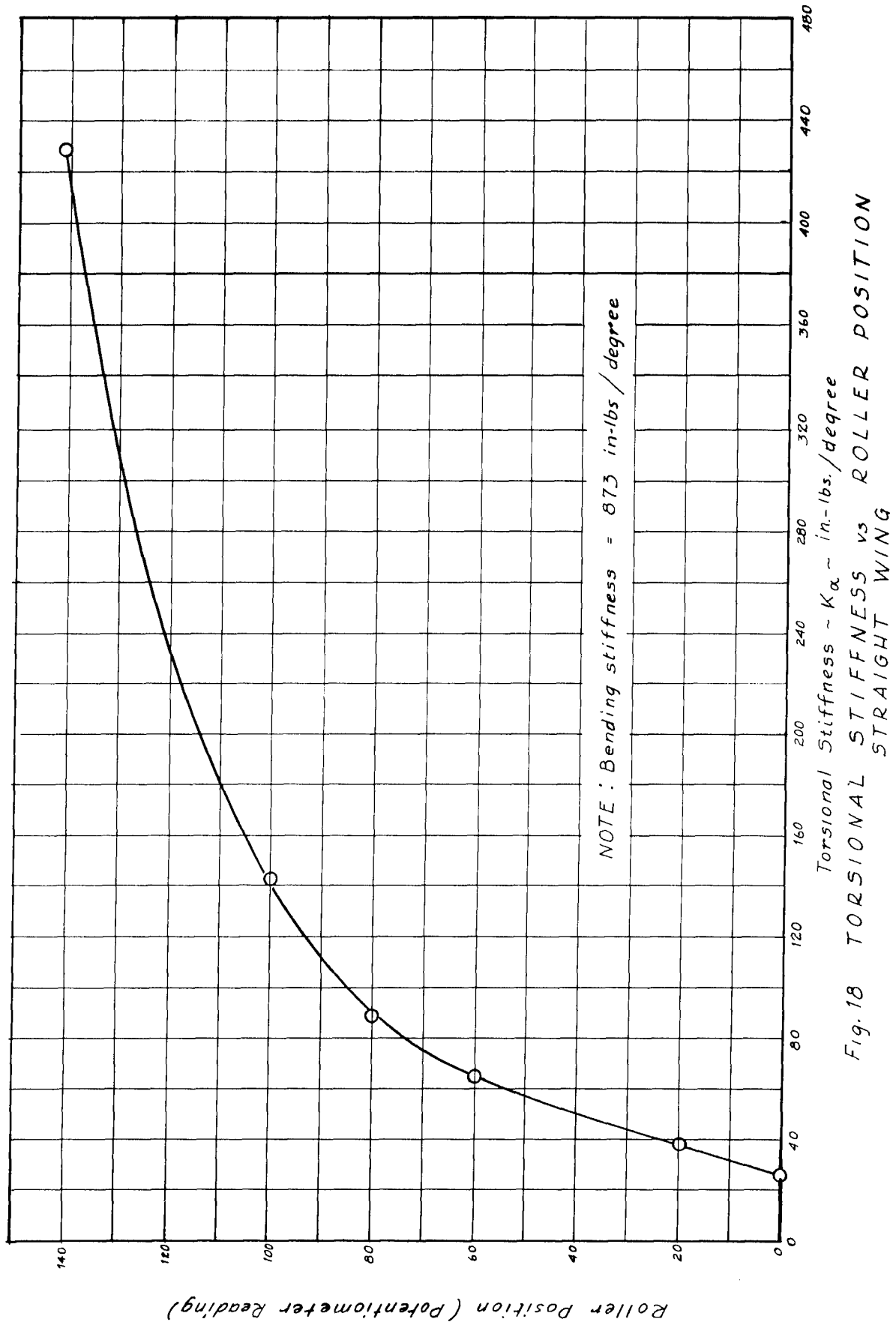


Fig. 17 - DISTRIBUTION OF C_L DUE TO AILERON DEFLECTION SWEPT WING

RESTRICTED

RESTRICTED



WADCTR 52-231

30
RESTRICTED

RESTRICTED

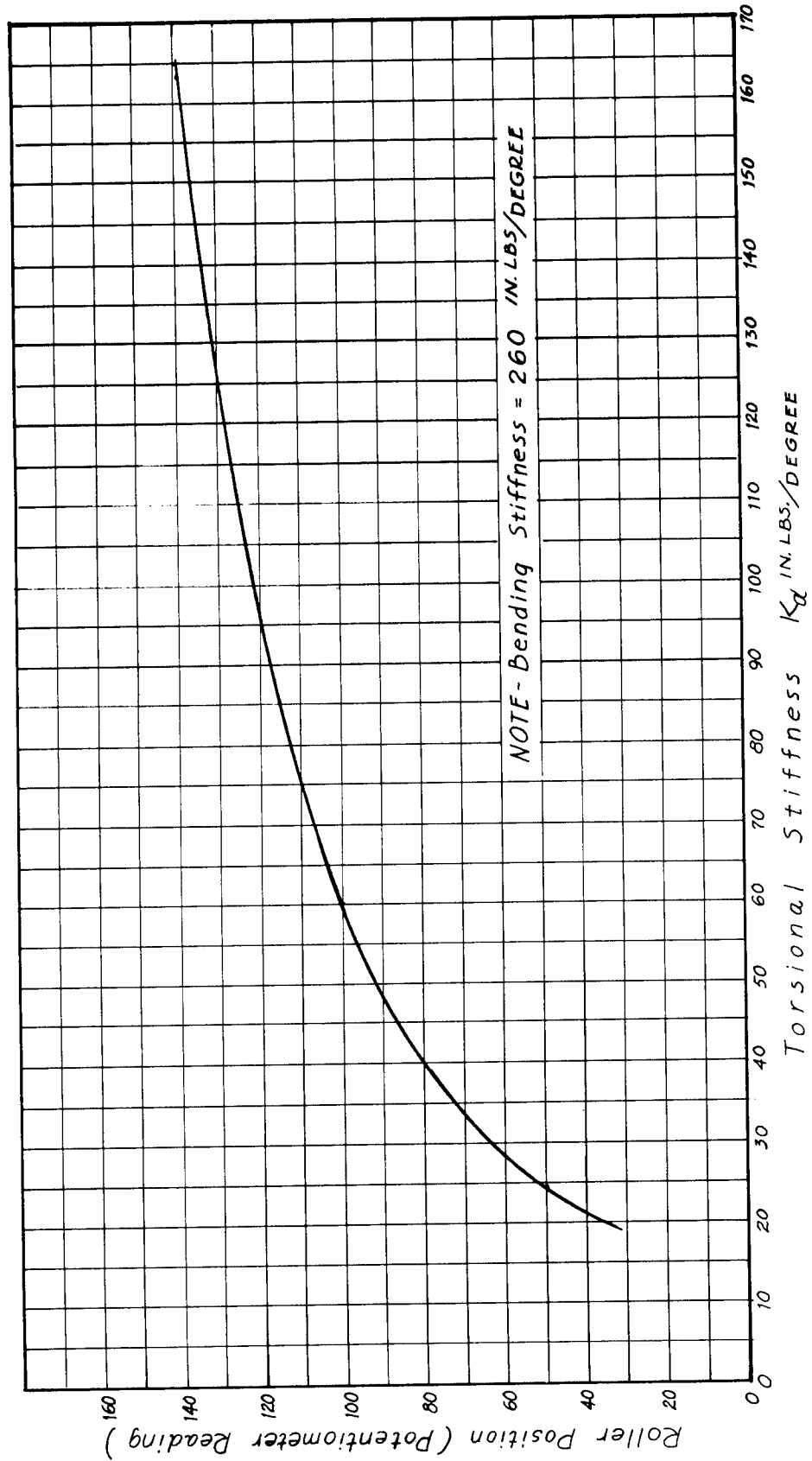


Fig. 19 - TORSIONAL STIFFNESS vs. ROLLER POSITION
SWEEP WING

RESTRICTED

RESTRICTED

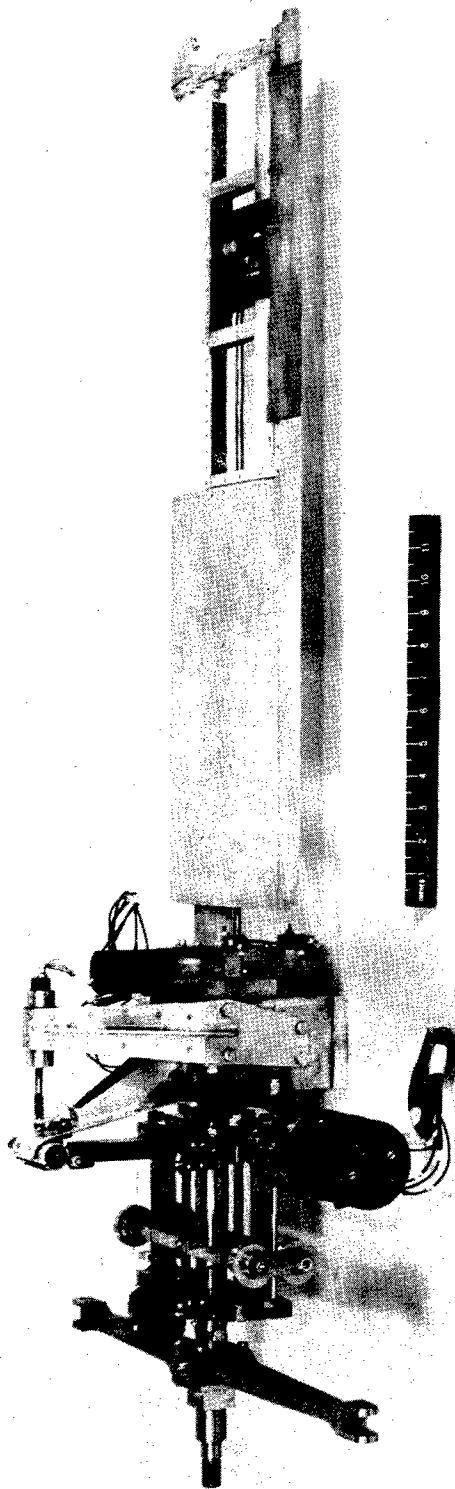


Fig. 20
STRAIGHT WING MODEL ASSEMBLY

WADCTR 52-231

32

RESTRICTED

RESTRICTED

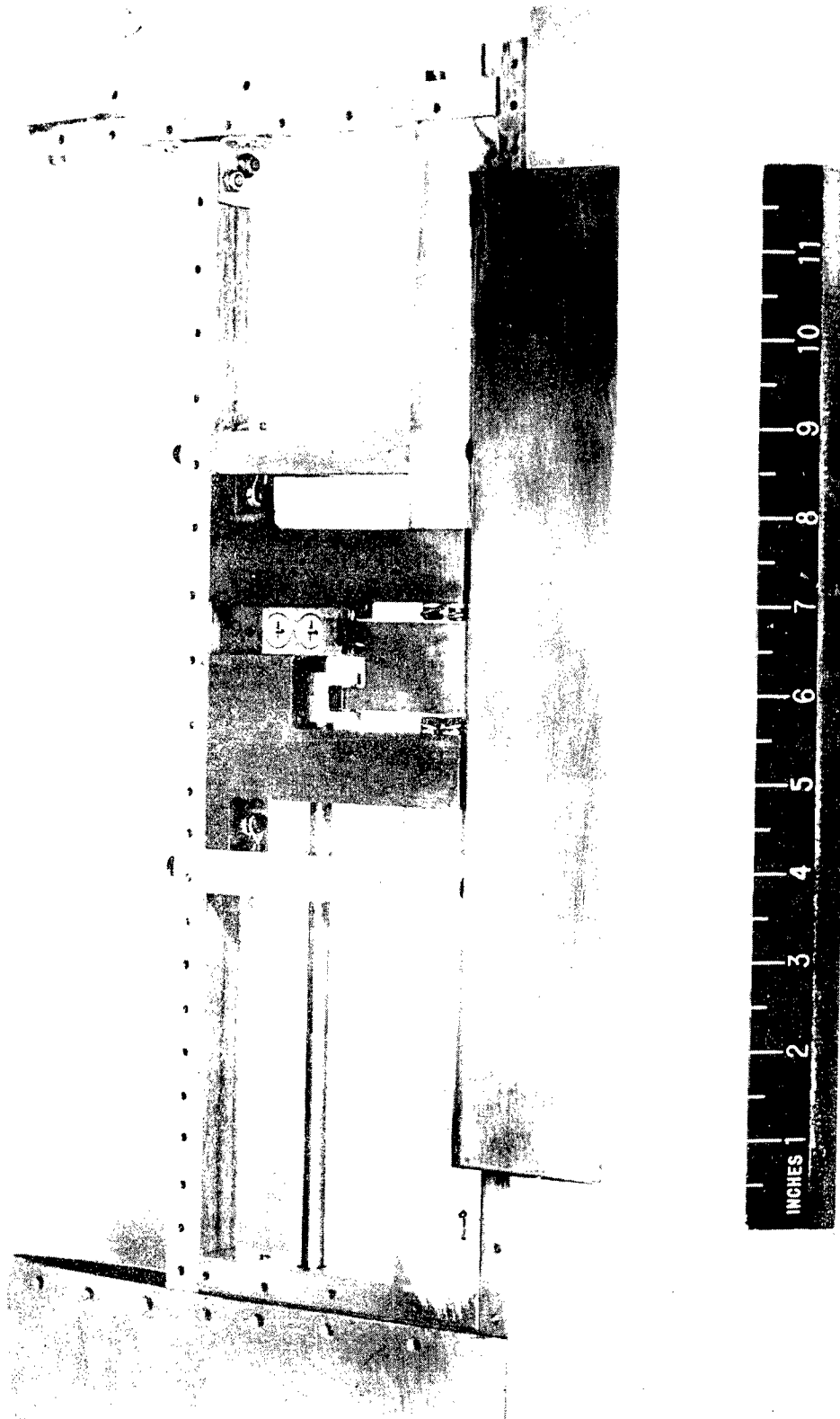


Fig. 21
AILERON CONTROL ASSEMBLY STRAIGHT WING

RESTRICTED

RESTRICTED

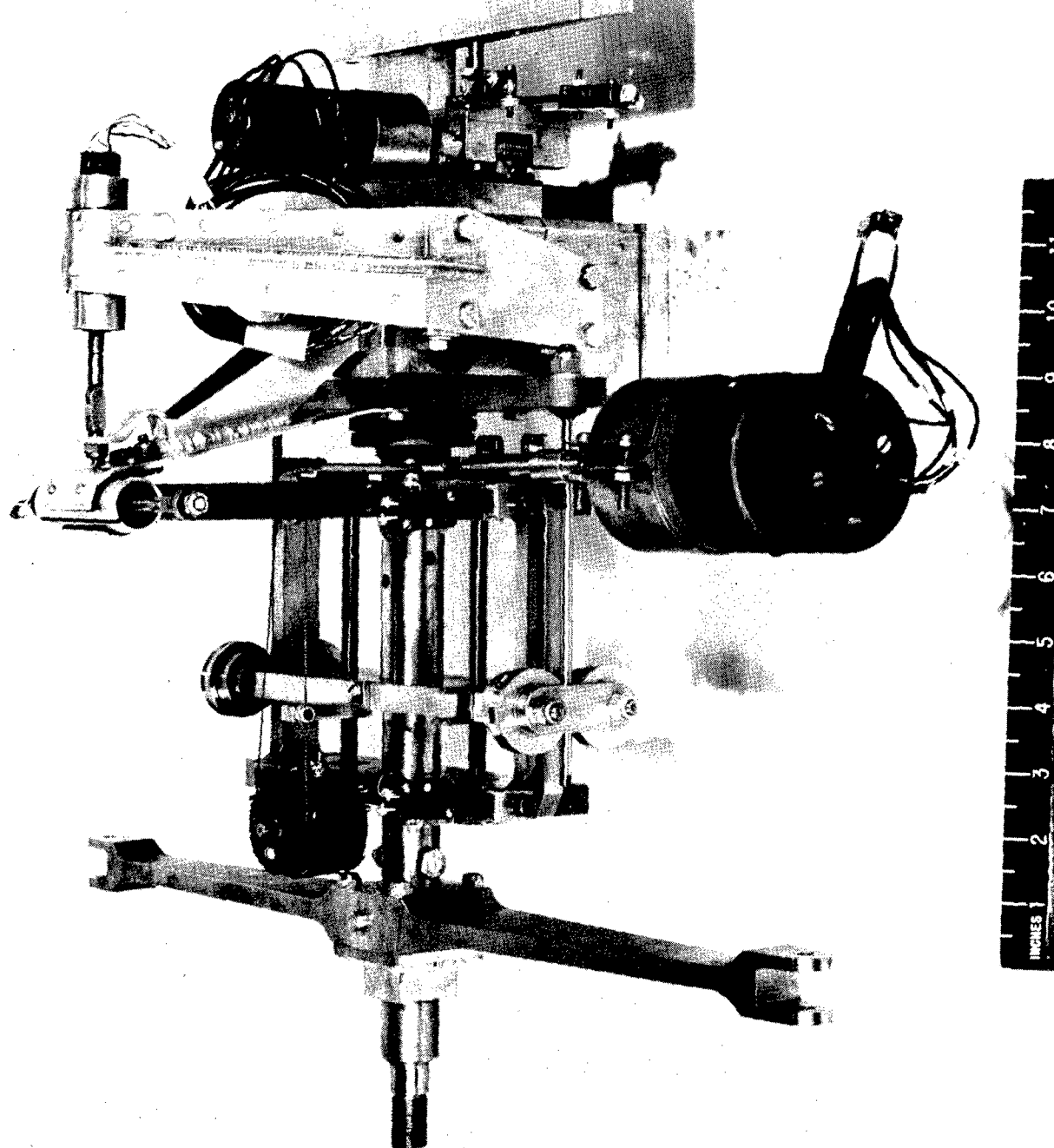


Fig. 22
VARIABLE TORSION SPRING ASSEMBLY,
AILERON CONTROL MOTOR, SCHAEFFERT ASSEMBLIES

WADCTR 52-231

34
RESTRICTED

RESTRICTED



Fig. 23
STRAIGHT WING MODEL MOUNTED IN WIND TUNNEL

WADCTR 52-231

35

RESTRICTED

RESTRICTED

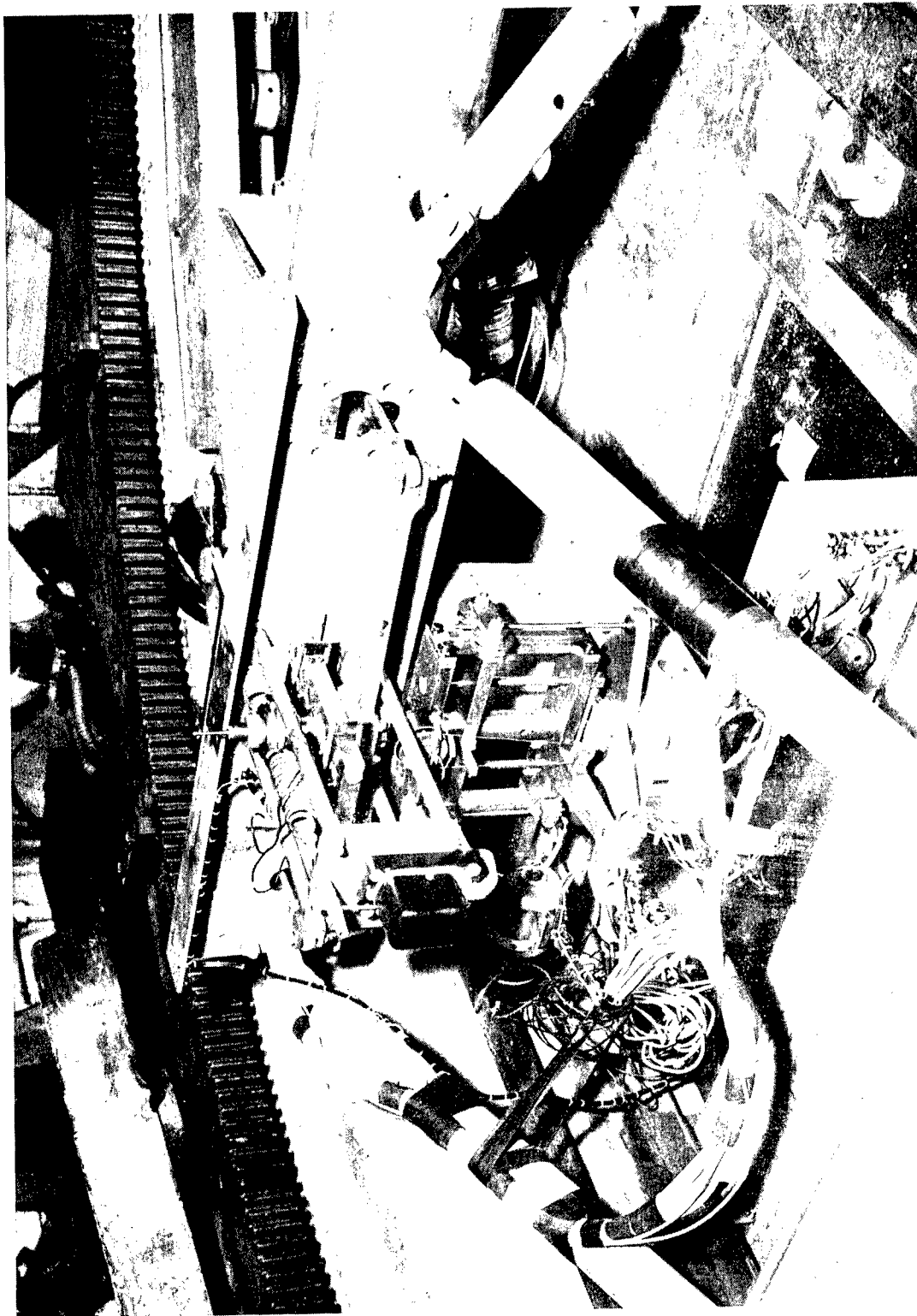


Fig. 24
TOP VIEW OF WIND TUNNEL CEILING WITH STRAIGHT WING MODEL INSTALLED-

WADCTR 52-231

36

RESTRICTED

RESTRICTED

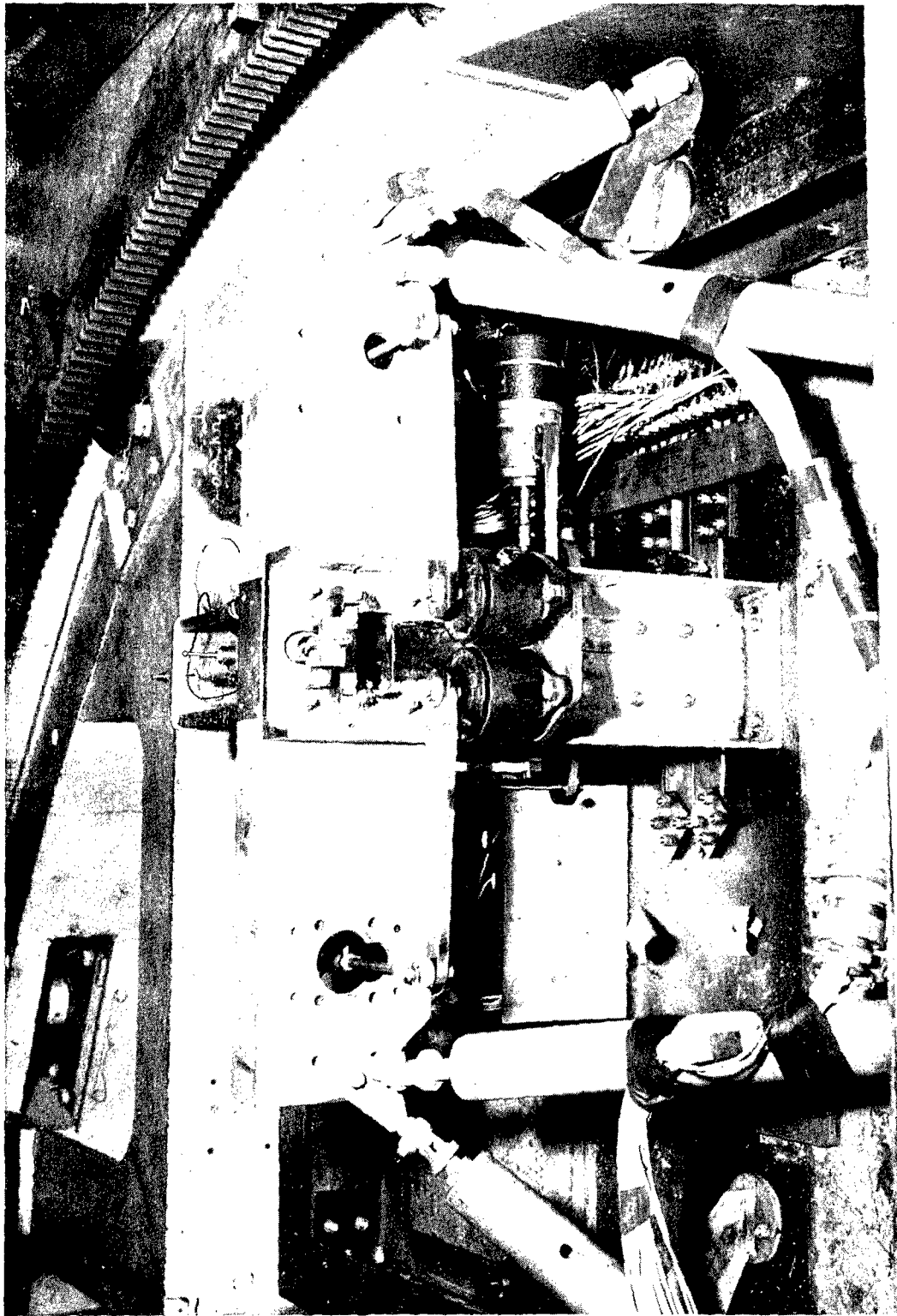


Fig. 25
TOP VIEW OF WIND TUNNEL CEILING WITH STRAIGHT WING MODEL INSTALLED-II

WADCTR 52-231

37

RESTRICTED

RESTRICTED



Fig. 26
SWEEP WING MODEL MOUNTED IN WIND TUNNEL

WADCTR 52-231

38

RESTRICTED

RESTRICTED

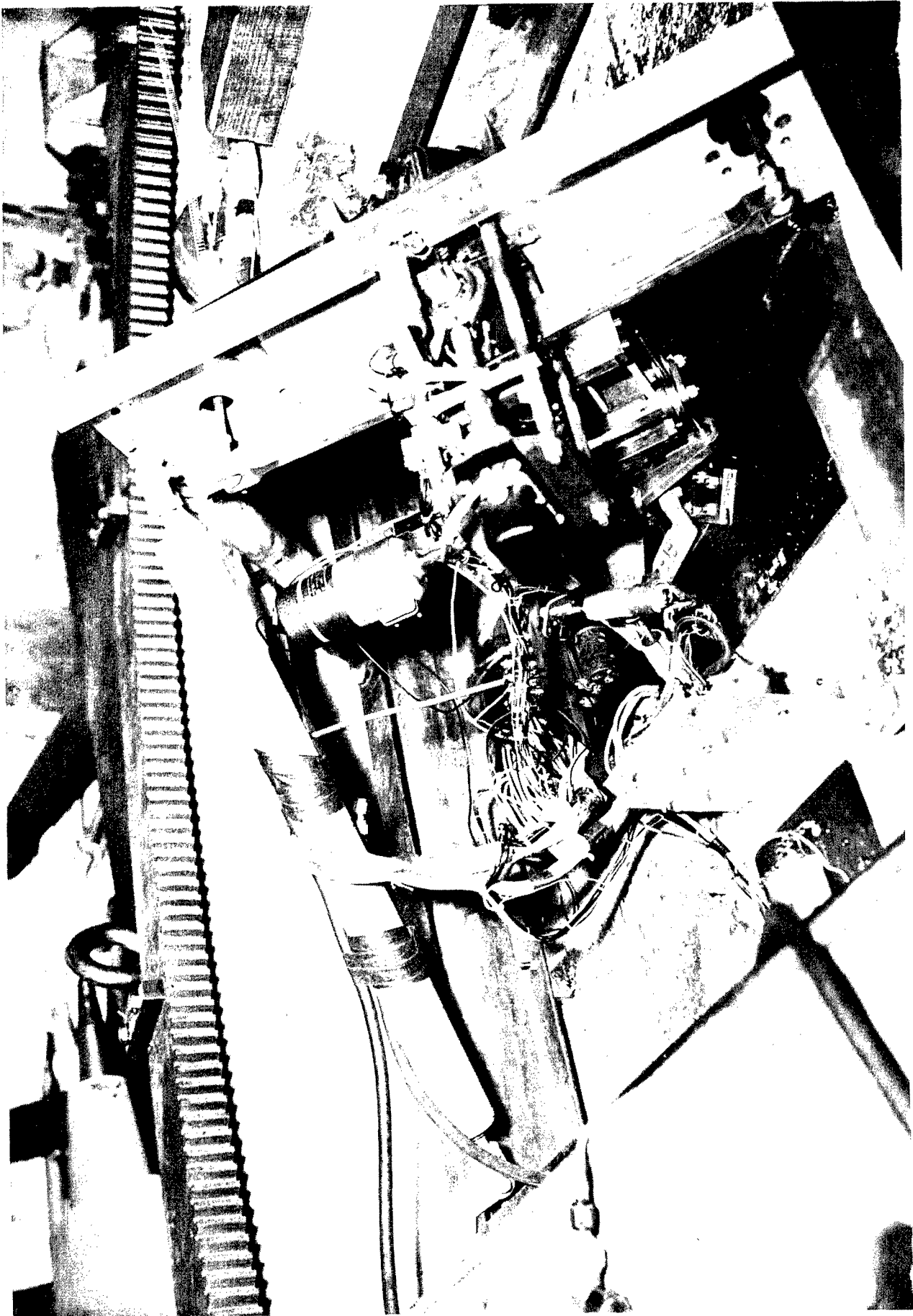


Fig. 27
TOP VIEW OF WIND TUNNEL CEILING WITH SWEEP WING MODEL INSTALLED-I

RESTRICTED

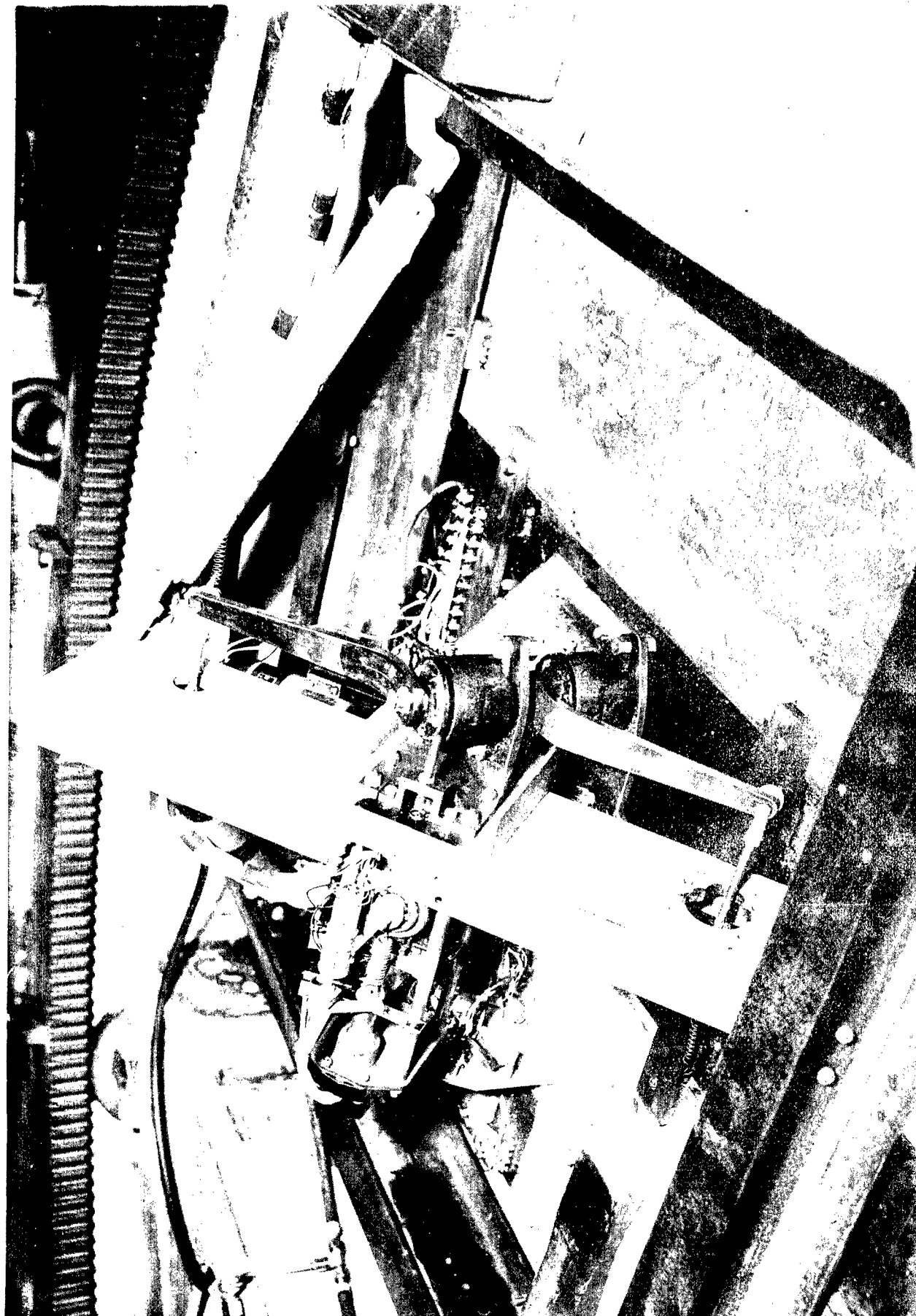


Fig. 28
TOP VIEW OF WIND TUNNEL CEILING WITH SWEEP WING MODEL INSTALLED-II

WADCTR 52-231

40

RESTRICTED

~~RESTRICTED~~

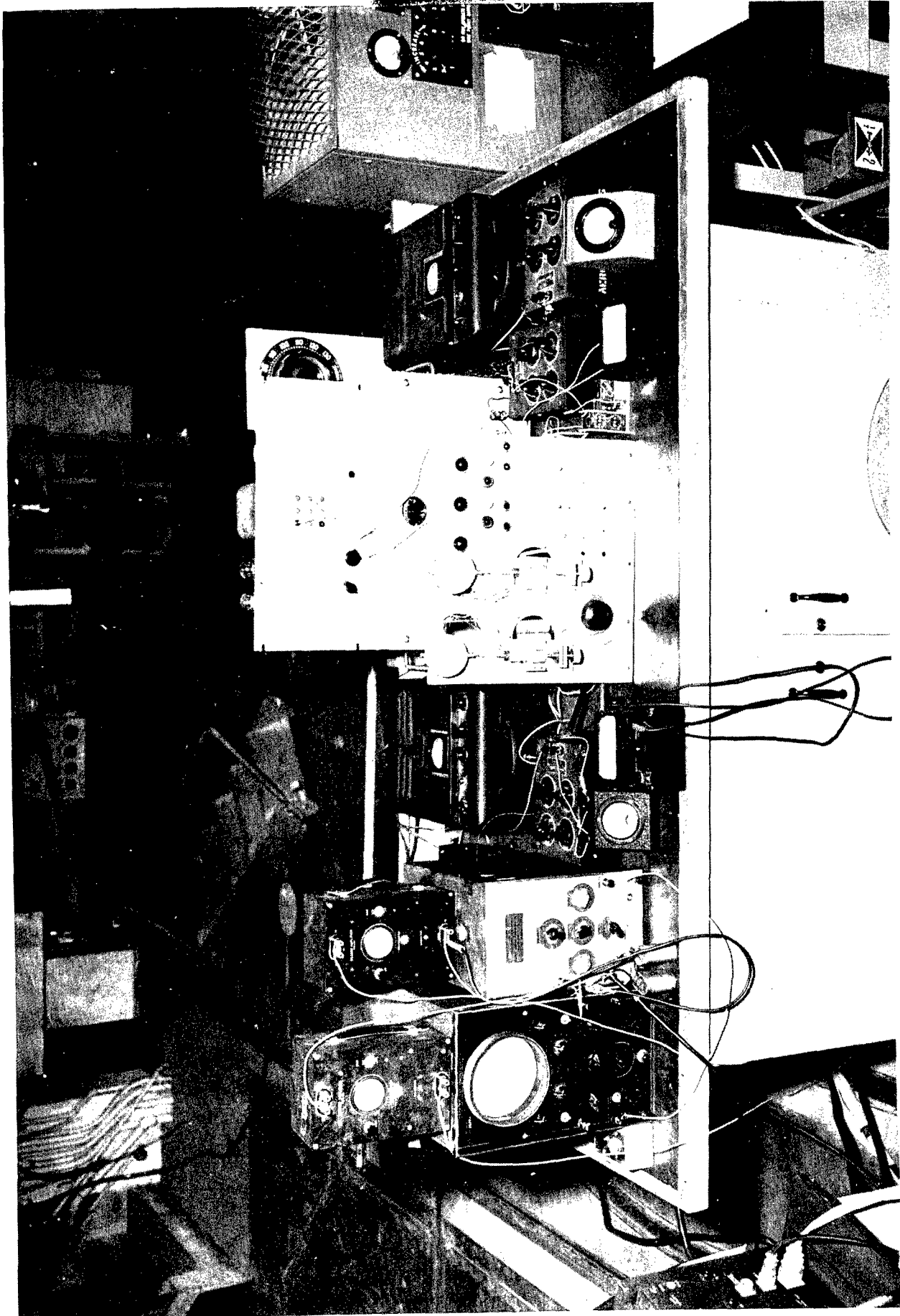


Fig. 29
LAYOUT OF INSTRUMENTATION

~~RESTRICTED~~